

1
2
3 **Impact of climate and land degradation on soil carbon fluxes in**
4 **dry semiarid grasslands in SE Spain**
5

6 Ana Rey⁽¹⁾, Luis M. Carrascal ⁽¹⁾, Carlos García-Gutiérrez Báez⁽²⁾, João Raimundo⁽³⁾,
7 Cecilio Oyonarte⁽⁴⁾, Emiliano Pegoraro^(*)
8
9
10

11 (1) National Museum of Natural Science (MNCN), Spanish Scientific Council (CSIC), C/ Serrano
12 115bis, 28006 Madrid, Spain

13 (2) Department of Mathematics, Polytechnic University of Navales, Av. Arco de la Victoria, 4. 28040
14 Madrid, Spain.

15 (3) Centre for Functional Ecology, Department of Life Sciences, University of Coimbra, Calçada
16 Martins de Freitas, 3000-456 Coimbra, Portugal

17 (4) Department of Agronomy, University of Almería, E-04120 La Cañada (Almería), Spain

18 (*) deceased
19

20 **Corresponding author:** anareysimo@gmail.com Phone: 0034 91 7452500 Fax: 0034 91 5668960
21
22

23 **Acknowledgements**

24 This work was funded by the Ministry of Education and Science (project CARBOARID, CGL2005-00563)
25 and the Instituto Nacional de Investigaciones Agrarias (project SUM2006-00018-C02-01). We thank the
26 Cabo de Gata Natural Park for supporting the research. We also thank Mrs. Claire Jasinski for proof reading
27 the manuscript. The study was originally thought as part of the project of a Marie Curie fellowship granted to
28 Dr. Emiliano Pegoraro who passed away before completion. This work is dedicated to him.
29

30 **Keywords:** soil CO₂ efflux, biological soil crust, Mediterranean dry grasslands, seasonality, degraded
31 grasslands, abiotic drivers, climate change, precipitation, temporal autocorrelation.
32
33

34 **Abstract**

35 **Aims.** This study investigates how precipitation, temperature and seasonality (as a proxy
36 of plant productivity) affect the temporal and spatial variability of soil CO₂ efflux in two
37 dry semiarid grasslands with different degrees of land degradation.

38 **Methods.** We measured soil CO₂ efflux over four years under plant, biological soil crust
39 and bare soil patches and estimated annual soil carbon losses in both, a natural and a
40 degraded grassland, by means of generalised additive mixed models considering temporal
41 autocorrelation in the data.

42 **Results.** Soil CO₂ efflux ranged from 0.08 to 3.70 and from 0.10 to 3.01 $\mu\text{mol CO}_2 \text{ m}^{-2} \text{ s}^{-1}$
43 in the natural and degraded grasslands, respectively. Daily soil CO₂ efflux was mostly
44 affected by moisture in the degraded grassland (25.4%), while in the natural grassland was
45 affected jointly by seasonality, temperature and moisture (27.5%). Overall, the highest soil
46 carbon fluxes were measured in soils covered by biological soil crusts (1.24 ± 0.02 and
47 1.10 ± 0.02) and the lowest in bare soils (1.11 ± 0.02 and $0.82 \pm 0.02 \mu\text{mol CO}_2^{-2} \text{ s}^{-1}$) in
48 the natural and degraded sites, respectively. Cumulative soil carbon fluxes were mainly
49 driven by temperature and previous precipitation (over three months). The highest soil
50 carbon losses were estimated in the driest year (2009) and the lowest in the wettest (2010)
51 with almost twice the amount of rainfall. The main difference between these years was the
52 timing of the events that mostly occurred in the moments of maximum plant activity with
53 optimum temperatures in spring in the dry year.

54 **Conclusions.** Changes in precipitation patterns will affect soil carbon fluxes more than
55 rainfall amount, particularly in degraded grasslands. Therefore, considering all climate
56 drivers together with plant activity is essential to predict how climate change will affect
57 soil biological processes in drylands.

58

59 **Abbreviations**

60 VEG: under plant cover BS: bare soil BSC: biological soil crust SR: soil CO₂ efflux

61 **Introduction**

62 Soil CO₂ efflux is the largest flux of CO₂ from terrestrial ecosystems with 68-98 Pg C
63 released to the atmosphere annually (Bond-Lamberty & Thomson 2010; Zhao et al. 2017),
64 and the second largest amount in the global carbon balance after that released by oceans
65 (IPCC 2014). Furthermore, soils constitute the largest terrestrial carbon pool with global
66 estimates of *ca.* 2456 Pg (Scharlemann et al. 2014). Despite intensive research over the last
67 two decades (see Bond-Lamberty & Thomson, 2010; Vargas et al. 2011; Rey 2015), we
68 still have a limited understanding of the controlling factors determining the temporal
69 variability of soil CO₂ effluxes across ecosystems (Reichstein & Beer 2008; Huang et al.
70 2020), particularly drylands. Drylands (arid and semi-arid ecosystems) occupy more than
71 40% of the surface of the Earth (Schimel 2010) and are responsible for the inter-annual
72 variability in the terrestrial carbon sink (Ahlström et al. 2015). These regions are
73 characterised by scarce and highly variable temporal distribution of rainfall. Thus, water
74 availability is an essential factor driving biological activity in these ecosystems. Rainfall
75 patterns (i.e. frequency, magnitude and timing of events) determine the temporal
76 variability of soil moisture and in turn, the biological activity in soils. Since most of the
77 carbon in semiarid grasslands resides in soils (Burke et al. 2008), predicted changes in
78 precipitation patterns could result in further soil carbon losses and land degradation (Smith
79 2011).

80 Some studies have quantified the relative contribution of rain driven carbon fluxes for the
81 ecosystem carbon balance demonstrating that they can be important in determining the
82 high inter-annual variability in the carbon sink capacity of these ecosystems (e.g. Jarvis et
83 al. 2007; López-Ballesteros et al. 2015). Over the last few decades, this phenomenon has
84 prompted increasing interest since climate change predictions for these regions include
85 changes in precipitation patterns with prolonged drought periods and more intense rainfall

86 events and climate extremes (Smith 2011; Greve et al. 2014). However, results on the
87 impact of intra-annual variation of precipitation distribution on soil carbon fluxes are still
88 inconclusive (Knapp et al. 2008; Fay 2009; Liu et al. 2019). Precipitation interacts with
89 temperature and in turn, with plant activity. Since the factors controlling soil CO₂ efflux
90 are often correlated, only apparent relationships can be obtained in field studies.
91 Experimental studies often manipulate environmental conditions in order to assess
92 individual factors such as precipitation or temperature (e.g. Rey et al. 2017; Arredondo et
93 al. 2018; Zhang et al. 2019; Manzoni et al. 2020). Another approach is to assess individual
94 effects by using ad hoc statistical approaches that take into account these correlations.

95 Besides high temporal variability in biological activity, these ecosystems are also
96 characterised by large spatial variability, with the presence of sparse vegetation patches,
97 biological soil crust and bare soil (Maestre et al. 2013). Vegetation patches represent
98 islands of nutrient availability, high root density and carbon pools. Moreover, plants
99 modify the energy and water balances as well as the amount and quality of soil organic
100 matter. The translation of rainfall into soil moisture, with subsequent impacts on soil
101 activity, is likely to be affected by ecosystem properties such as vegetation cover, presence
102 of biological soil crusts, and soil texture (Cable et al. 2008; Zhang et al. 2008). Biological
103 soil crusts are globally widespread communities (cyanobacteria, green algae, lichens and
104 mosses) that may constitute a large proportion of the living cover in drylands (Belnap &
105 Lange 2003). These communities play an important role preventing soil erosion, improving
106 soil stability and fertility, and contributing to carbon uptake and nitrogen fixation (Li et al.
107 2018). Castillo-Monroy et al. (2011) found that biological soil crusts accounted for 43% of
108 the total carbon released via soil respiration in a semiarid steppe in Spain. As biological
109 soil crusts live on the soil surface, they get activated even by small precipitation events and
110 high relative humidity (Li et al. 2018). Thus, factors determining soil CO₂ efflux from

111 different ground covers are likely to differ and may respond differently to rainfall events
112 and environmental variables, which may have potential consequences for soil and
113 ecosystem functioning (Borken & Matzner 2009). The high spatial heterogeneity of
114 vegetation and soil properties in drylands makes soil CO₂ efflux particularly difficult to
115 quantify.

116 Despite the recognised importance of precipitation and temperature as main abiotic drivers
117 of biological activity, a proper characterisation of other factors controlling soil carbon
118 fluxes, considering the spatial variability of soil CO₂ efflux characteristic of drylands and
119 the importance of plant activity, is still lacking (Leon et al. 2014; Nielsen & Ball 2015).

120 While the effect of single precipitation events on soil CO₂ efflux has been fairly well
121 studied (e.g. Cable et al. 2008; Chen et al. 2008; Aanderud et al. 2011; Rey et al. 2017),
122 few studies have examined long-term responses of soil carbon fluxes over several years to
123 precipitation in the field. Moreover, most of the published studies have been carried out in
124 ecosystems with mean annual precipitation above 300 mm (e.g. Correia et al. 2012), but
125 studies examining the response of ecosystems located in more extreme climates are very
126 scarce (e.g. Zhang et al. 2010). Therefore, it is crucial to understand the impact of rainfall
127 amount, timing and distribution and temperature on soil carbon fluxes in more extreme dry
128 environments considering the spatial variability that characterise these ecosystems (Sitch et
129 al. 2008).

130 Furthermore, land degradation is threatening semiarid ecosystems, with more than 20% of
131 semiarid lands prone to desertification potentially affecting soil carbon dynamics (Reed et
132 al. 2012; Feng & Fu 2013). Land-cover change and land degradation greatly affect soil
133 CO₂ efflux by changing vegetation structure, local microclimate and soil properties
134 (Alekseev et al. 2018; Thomas et al. 2018). As soil carbon and nutrient availability, the
135 substrates of soil microbes, ultimately depend on photosynthate supply (Mitra et al. 2019),

136 it is important to consider plant productivity as another relevant factor influencing soil CO₂
137 efflux in these ecosystems. So far, few studies have considered how both climate and land-
138 cover change as a result of land degradation affect the spatial and temporal variability of
139 soil carbon losses (Huang et al. 2020). Thus, in order to predict how dryland carbon
140 dynamics will be affected by climate change, it is necessary to understand how changes in
141 vegetation and biocrust cover and soil impoverishment as a result of land degradation will
142 affect soil carbon fluxes in these regions.

143 In this study, we measured soil CO₂ efflux over almost four years in two nearby sites with
144 different degree of land degradation as a result of distinct land use history (see Rey et al.
145 2011) and in three representative soil covers: under vegetated areas, biological soil crust,
146 and bare soil patches. The overall aim of this study was to characterise the temporal and
147 spatial variability of soil CO₂ efflux rates. We used a statistical approach that allowed us to
148 disentangle the individual effects of environmental factors incorporating seasonality as a
149 proxy of plant productivity. Specific objectives were: (1) to examine the temporal
150 variability of soil CO₂ efflux in two dry semiarid grasslands with different degrees of land
151 degradation, (2) to investigate the spatial variability of soil CO₂ efflux by exploring how
152 the response to environmental variables is modulated by different soil covers, (3) to assess
153 the impact of land degradation on soil CO₂ efflux and soil carbon losses since it can affect
154 biocrust cover and composition and, (4) to understand to what extent rainfall and
155 temperature determine inter-annual variability of soil carbon fluxes, taking into
156 consideration seasonality as a proxy for plant productivity. The final aim is to understand
157 how changes in precipitation patterns and increasing temperatures will affect soil carbon
158 losses via soil CO₂ efflux in these dry ecosystems, including degraded lands. We
159 hypothesised that in these semiarid dry ecosystems: (1) the temporal variability in soil CO₂
160 efflux rates will be very large and mediated by plant productivity since the translation of

161 rainfall into soil moisture will depend on plant activity, (2) since moisture is the main
162 limiting factor in these ecosystems, we expect the highest soil CO₂ fluxes from biological
163 soil crusts given that they get activated by small to large rainfall events and high relative
164 humidity, (3) since land degradation leads to lower vegetation cover, changes in biocrust
165 cover and composition and large percentage of bare soil patches, we also expect further
166 carbon losses from soils in the degraded grassland, (4) although we expect that
167 precipitation will be the main factor controlling biological activity in these ecosystems, the
168 combination of precipitation, temperature and productivity will determine how
169 precipitation converts into soil moisture and thus will determine soil CO₂ effluxes in these
170 dry semiarid grasslands.

171

172 **Material and Methods**

173 *Site description*

174 We selected two sites in the Cabo de Gata Natural Park, in the province of Almería
175 (Andalucía) in the SE of Spain (N 36° 56' 26.0'', W 2° 01' 58.8''). The climate in this area
176 is semiarid with a mean annual precipitation of 200 mm and a mean annual temperature of
177 approximately 18°C (nearby meteorological station, Níjar). The area is characterised by
178 prolonged summer droughts (from May to September) and strong inter-annual variation
179 and random patterns of precipitation, which mostly occur in spring and autumn.
180 Geologically, the region is a series of alluvial fans (glacis) with gentle slopes (2 to 8%)
181 with petrocalcic horizons. The dominant soils are classified as Lithic leptosols (calcaric)
182 (WRB 2006), and are thin (on average 10 cm), alkaline (pH above 8), with a sandy loam
183 texture in both sites, saturated in carbonates with a moderate stone content and with
184 common rock outcrops, particularly at the degraded site (Supplementary material S1, S2).
185 The vegetation of these sites is dominated by *Stipa tenacissima*, but there are a large

186 number of other shorter grass species with low ground coverage (Supplementary material
187 S2), such as: *Chamaerops humilis*, *Rhamnus lycioides*, *Asparagus horridus*, *Olea europea*
188 var. *sylvestris*, *Pistacia lentiscus*, and *Rubia peregrina*.

189 The two sites are located approximately 15 km apart on a flat area. The natural grassland is
190 called Balsablanca and is located over a flat terrain 200 m a.s.l.; whereas the other site,
191 Amoladeras, is located at 50 m a.s.l, with less vegetation cover and shallower soils (see
192 Supplementary material S1 and S2).

193 Based on a previous hierarchical classification of the ecosystems present in the Cabo de
194 Gata Natural Park (see Escribano, 2002), we selected the two sites as representative of two
195 distinctive degradation stages as a result of distinctive land use history (Rey et al. 2011)
196 making sure that both sites were comparable with the same geology, topography,
197 vegetation type, climate, etc., and consistent with a soil cartography map (CMA, 1999).
198 This analysis indicated that soils in the degraded grassland (Amoladeras) have
199 characteristics typical of degradation processes as a result of past overgrazing, in
200 comparison to soils in the natural grassland (Balsablanca) that remains unmanaged. Other
201 degradation indicators such as the percentage of vegetation cover, rock outcrops, and
202 surface coarse fragments were also used (Cammeraat 1996; Dregne 2002). Thus, even
203 though the sites are 15 km apart, they represent different degrees of ecosystem
204 degradation.

205

206 *Experimental design*

207 In December 2006, we selected six permanent replicated plots at both sites within a 100 m
208 fetch of the eddy covariance tower. Plots measured 10 m by 10 m and were at least 5 m
209 apart. Vegetation was mainly patchy, with different percentage of plant cover at each site
210 (Supplementary material S1). In each plot, we selected three representative soil covers and

211 placed three soil collars (15 cm in diameter and 7 cm in height) inserted 3.5 cm into the
212 soil at three different locations: *under plant cover* (VEG), at 40-50 cm from the plants on
213 *bare soil* (BS), and over *biological soil crust* (BSC). The plant cover is *Stipa* spp., the
214 dominant grass species (63% and 23% cover in the natural and degraded sites,
215 respectively). The experimental design is defined by 36 replicated sampling collars
216 representing three soil types in two areas differing in land degradation.

217

218 *Soil CO₂ efflux and environmental measurements*

219 We measured soil CO₂ efflux (SR) from January 2007 until August 2010 at a frequency of
220 approximately one to two weeks, depending upon the time of year (more frequent in spring
221 and autumn). In order to capture the short-term response to rainfall, we tried to measure
222 soil CO₂ efflux after each rainfall event over the whole duration of the experiment, thus,
223 also under changing humidity conditions. After placing the soil collars and during the
224 entire duration of the study, small plants, litter, insects, and grasses were regularly and
225 carefully removed from each soil collar. To avoid strong diurnal fluctuations,
226 measurements were made between 10:00 and 14:00 h at both sites on alternative
227 consecutive days. We measured diurnal courses of soil CO₂ efflux at different times of the
228 year representative of four seasons in order to adjust the measurements to average diurnal
229 values (Supplementary material S3). Plots were measured in random order on each date to
230 avoid biased estimates. A portable, closed chamber, soil respiration system (EGM-4, PP-
231 systems, MA, USA) was used to measure soil CO₂ efflux rates *in situ*. The chamber
232 covered an area of 78 cm² and had a volume of 1170 cm³. Because of the low rates of soil
233 CO₂ efflux, each measurement period was 90 s to ensure reliable measurements. Given the
234 presence of thin soils, we measured soil temperature and soil water content at 3.5 cm at

235 each measuring time with a soil thermistor and a portable soil moisture sensor (Field Scout
236 TDR 300 Soil Moisture Meter, Spectrum Technologies, Inc., Illinois, USA), respectively.

237

238 *Statistical analyses*

239 Generalised additive mixed models (GAMM hereafter; Wood 2006) were used to analyse
240 the variation of soil CO₂ efflux throughout the study years. GAMMs are based on
241 smoothing techniques aimed to identify non-linear trends in data without adopting strong
242 assumptions about the specific nature of these relationships (e.g., linearity). As soil CO₂
243 efflux was measured on 90 different days not evenly spaced throughout time, we used a
244 continuous-time first-order autoregressive correlation structure (corCAR1) to account for
245 the non-independence temporal serial data, using date as a continuous time covariate. The
246 effect of the time covariate was nested within each sampling point, thus not assuming a
247 common temporal pattern across the 36 sampling collars. In order to account for the
248 seasonality effect in temporal data, we converted the 365 days of the year to 360 degrees
249 (Zar 1999), considering that 0° and 360° correspond to winter solstice (21st December),
250 180° relates to summer solstice (21st June), and 90° and 270° define the spring and autumn
251 equinoxes, respectively. Once time position within an annual cycle was established (i.e.,
252 angular date), the cosine and sine of that angular transformation were obtained (cosine and
253 sine are perfectly orthogonal). As soil CO₂ efflux was measured in each collar throughout
254 the study years, these 36 sampling collars establish the random effect. Soil water content,
255 soil temperature, the cosine and sine of the angular transformation of date, rainfall amount
256 and rainless duration were included in the GAMMs as fixed covariates, while land
257 degradation (two levels) and soil cover (three levels) were considered as fixed factors. We
258 used penalised thin plate regression splines with the individual predictors in the GAMMs,
259 setting the maximum complexity dimension of the smooth (k) to four. A tensor product

260 smoothing term (i.e., additive regression plane) was used for the seasonal terms cosine and
261 sine of the angular transformation of date, setting the maximum complexity dimension of
262 the smooth ($k \times k$) to seven (maximum of $7 \times 7 = 49$). The relatively low maximum
263 complexity dimension k was established in order to reduce over-fitting of the splines to the
264 data (thus avoiding over-parametrisation in response to local minima/maxima), without
265 much degradation in prediction error performance. The final model of interest was
266 obtained using restricted maximum likelihood estimation (REML).

267 GAMMs were run using the `gamm` command of the `{mgcv}` package in R (Wood 2017),
268 assuming a Gaussian distribution of errors (link function: identity). We checked for
269 normality and the lack of heteroscedasticity in the residuals of the final GAMM. To
270 accomplish these criteria, soil CO_2 efflux was log transformed prior to data analyses.

271 Since the effects of predictors may change across sites (degraded vs. natural), two different
272 GAMM models were built for soil CO_2 efflux: one for both sites together, and another
273 analysing the effect of soil temperature and soil water content nested within site. Both
274 models were compared using ML estimation and the sample-size corrected version of the
275 Akaike criterion (AICc).

276 Partial residual plots were obtained to show the effect of each predictor in the GAMM on
277 the response while taking into consideration the influence of the remaining predictors.
278 Finally, we built several reduced models from the full GAMM model to partition the
279 variance in the response variable and to decompose the explanatory capacity of predictors
280 into independent and shared components through variation partitioning (Legendre &
281 Legendre 1998). Significance of post-hoc Student t -tests comparing partial residuals of soil
282 CO_2 efflux rates among soil covers (derived from the corresponding GAMM) were
283 obtained using the false discovery rate adjustment method of the `p.adjust` function in R

284 (i.e., controlling the rejection of the null hypothesis when it is false). All analyses were
285 carried out with the statistical program R version 3.5.0 (R Core Team 2018).

286

287 *Annual estimates of carbon fluxes from soils*

288 In order to estimate annual carbon losses via soil CO₂ efflux as well as the factors
289 controlling the seasonal variability in soil carbon fluxes, we calculated the amount of
290 carbon released (g C m⁻²) every fortnight from each soil cover at each site by interpolating
291 measurements between sampling dates over the study period. Given the high frequency of
292 measurements, the estimates can be considered fairly robust and comparable between sites.
293 For each study site, we estimated the weighted average of soil carbon loss of all replicates
294 considering the soil cover area of each soil cover type (Supplementary material S1 and S3).
295 This interpolation was carried out using GAMMs where the only predictor was the thin
296 plate spline of sequential date beginning on January 1st 2007 and ending on June 30th 2010
297 (using k=87 as the dimension of the basis used to represent the smooth term). The same
298 approach was repeated to obtain interpolations of the soil temperature and soil water
299 content every day throughout the study period. All models accounted for an extremely high
300 proportion of deviance (always > 70% for the six combinations of two sites and three soil
301 covers). The predicted-interpolated soil carbon loss was estimated by means of the
302 summation of the interpolated rates over the 15 days. The predicted-interpolated soil
303 temperature and soil water content were estimated by means of the average of the
304 interpolated rates over the 15 days (Supplementary material S4). Although manual
305 measurements done periodically may miss some temporal variability, the frequency in this
306 study was high enough to characterise the temporal variability in soil CO₂ efflux. Daily
307 predicted values for each variable were averaged (soil water content and soil temperature)

308 or summed up (precipitation and soil carbon loss) over fortnights. Thus, the sampling units
309 are the fortnight values in the analyses accounting for the seasonal rainfall patterns.

310 Data for soil carbon losses were corrected to obtain mean daily totals based on
311 measurements done between 10 am and 2 pm, according to diurnal measurements made in
312 each soil cover in four seasons (see Supplementary material S3). This correction is needed
313 because soil CO₂ efflux rates at midday were considerably higher (winter) or lower
314 (summer) than that measured for a whole day. In other words, predicted-interpolated data
315 for midday soil CO₂ efflux rates in each soil cover were divided by proper correction
316 indexes in order to scale up for the whole 24 h. Correction figures (i.e., divisors of 10-14 h
317 soil CO₂ efflux rates) ranged between 1.41 and 2.57, depending upon soil cover and
318 season. Although this correction is only an approximation which may have caused some
319 under/overestimation, the comparison between sites and correlation with different
320 predictor variables should be valid.

321 We applied a GAMM model assuming a Gaussian distribution of errors (link function:
322 identity) to analyse the seasonal variation in soil carbon loss using the fortnight as the
323 sample unit (N=80), grassland degradation (site) as a fixed factor, and the mean *soil*
324 *temperature* and *precipitation* as continuous predictor variables. We also used temporal
325 autoregressive correlation structure to account for the non-independence temporal serial
326 data, using the fortnight as a continuous time covariate. We tested several time lags for
327 accumulated rainfall (fortnight, 1, 2, 3 and 4 months) using ML estimation. The most
328 parsimonious model (i.e. lower AICc) was the one including the accumulated amount of
329 rainfall over the previous three months. The final model was carried out using REML
330 estimation.

331

332

333 **Results**334 *Temporal dynamics of environmental variables and soil CO₂ efflux*

335 Environmental variables showed strong seasonality with warm and dry long summers and
336 wetter and colder winter periods (Figure 1). Environmental conditions significantly
337 differed ($P < 0.01$ in all cases) between both sites with warmer and drier conditions in the
338 degraded than in the natural grassland (Supplementary material S1, Figure 1). Soil
339 temperature ranged from 6.4 to 42.7°C with an average of 22.3°C, and from 8.4 to 43.5°C
340 with an average of 24.0°C for the natural and degraded grasslands, respectively. Soil water
341 content ranged from 0.7 to 52.6% (average of 15.3%) and from 0.3 to 41.0% (average of
342 11.7%) for natural and degraded grasslands, respectively.

343 Temporal variability in soil CO₂ efflux showed strong seasonality ranging from 0.08 to
344 3.70 $\mu\text{mol CO}_2 \text{ m}^{-2} \text{ s}^{-1}$ (average value of 1.19) and from 0.10 to 3.01 $\mu\text{mol CO}_2 \text{ m}^{-2} \text{ s}^{-1}$
345 (average value of 0.95) in the natural and degraded grasslands, respectively (Figure 1).
346 Soil CO₂ efflux rates varied similarly in all soil covers following temporal variation in
347 environmental variables (Pearson correlation between 0.83 and 0.95). However, temporal
348 fluctuations in soil CO₂ efflux were much larger than those observed for soil water content
349 and soil temperature.

350 Precipitation showed strong intra- and inter-annual variation. The year 2009 was the driest
351 (166 mm) and 2010 the wettest (364 mm) year. On average across all years, it rained 10%
352 of the days of the year. Although just 11% of the events were larger than 15 mm, these
353 events accounted for between 36% and 52% of total annual precipitation (Table 1). Apart
354 from very dry summers with practically no rain, rainfall varied among seasons from year to
355 year. Therefore, the study years differed considerably in rainfall amount and distribution
356 (Table 1).

357

358 *Factors controlling soil CO₂ efflux*

359 A model for soil CO₂ efflux including the effects of *soil water content* and *soil*
360 *temperature* nested within soil degradation attained a higher strength of evidence
361 (according to the lowest AICc value: -1224) than the model that generalised their effects
362 without distinguishing between levels of soil degradation (AICc = -1046; see
363 Supplementary material S5). Soil CO₂ efflux was a predictable and highly explainable
364 phenomenon (Table 2; likelihood ratio test: $\text{Chi}^2 = 1867$, $\text{df} = 16$, $P \ll 0.001$; $R^2 = 53.2\%$).
365 All effects in the model were highly significant ($P \ll 0.001$). An alternative model
366 including the two rainfall predictors (*rainfall amount* and *rainless duration*), instead of *soil*
367 *water content*, had a considerably lower strength of evidence than the previous model
368 (AICc = -254, $\Delta\text{AICc} = 971$; see Supplementary material S5), and accounted for a lower
369 proportion of variability in soil CO₂ efflux ($R^2 = 37.6\%$).

370 Variation partitioning of soil CO₂ efflux showed that the relative importance of the factors
371 determining soil CO₂ efflux differed between sites (Figure 2). *Soil water content* was the
372 main factor controlling soil CO₂ efflux in the degraded grassland (25.4%), while the
373 combined, correlated effect of *soil water content*, *soil temperature* and *seasonality* exerted
374 the largest control in the natural grassland (27.5%). Indeed, both *soil temperature* and
375 *seasonality* exerted much larger control on soil CO₂ efflux in the natural (19.1%) than in
376 the degraded grassland (9.4%).

377 Soil CO₂ efflux increased markedly with soil temperature up to 22°C almost linearly at
378 both sites. Above this value, soil CO₂ efflux remained constant in the degraded grassland,
379 and gently decreased in the natural grassland (Figure 3a). Soil CO₂ efflux increased with
380 soil water content at a higher rate up to *ca.* 15% in the degraded grassland and remained
381 significantly lower above 20% in the natural grassland. That is, high soil moisture values

382 (above 20%) led to higher soil CO₂ efflux rates in the degraded grassland than in the
 383 natural grassland (Figure 3b).

384 Soil CO₂ efflux showed a striking seasonal pattern, all other factors being equal: it reached
 385 the lowest levels around winter solstice, with the highest recorded values from spring
 386 equinox to summer solstice, when the activity of vegetation and biocrust was in its peak in
 387 the study area (see the smoothing seasonal pattern in Figure 3c). Finally, Figure 4 shows
 388 how soil CO₂ efflux was influenced by soil moisture and soil temperature at both sites.
 389 Maximum soil CO₂ efflux rates were measured in both areas at soil temperatures *ca.* 40 °C
 390 and soil water content *ca.* 40%. The influence of soil temperature was more marked (i.e.,
 391 higher slopes) in the natural than in the degraded grassland, while the influence of soil
 392 water content was more marked in the degraded grassland.

393

394 *Spatial variability in soil CO₂ efflux*

395 **Site** and **soil cover** had a very significant influence on soil CO₂ efflux other effects held
 396 constant (see Table 2 and Figure 5). The interaction term **soil cover*site** was also
 397 significant, indicating that the differences among the three soil covers changed between
 398 sites. The highest soil CO₂ efflux rates were measured in the biological soil crust (mean ±
 399 SE: 1.24 ± 0.02 and 1.10 ± 0.02 μmol CO₂ m⁻² s⁻¹ in the natural and degraded sites,
 400 respectively) and the lowest in bare soil (1.11 ± 0.02 and 0.82 ± 0.02 μmol CO₂ m⁻² s⁻¹ in
 401 the natural and degraded sites, respectively) at both sites, but differences were more
 402 pronounced in the degraded grassland (Figure 5a). Differences among soil covers, although
 403 highly significant ($P \ll 0.001$), accounted for only 4.6% of explained variation in the
 404 previous model. Adjusted soil CO₂ efflux (that is, controlling for the difference in soil
 405 temperature and soil water content among soil covers and sites) was higher in soils covered
 406 by biological soil crust and in bare soils in the natural than in the degraded grassland,

407 although this difference was larger in the bare soil cover (Figure 5b). Differences between
 408 sites disappeared ($F = 0.76$, $P = 0.385$) when soil CO₂ efflux rates were expressed on a soil
 409 carbon basis ($\text{mg C g C}^{-1} \text{ day}^{-1}$, Figure 5c). Nevertheless, soil cover remained significant (F
 410 $= 19.30$, $P \ll 0.001$). When soil CO₂ efflux was expressed on a carbon basis, the
 411 interaction term **soil cover*site** was not significant ($F = 1.04$, $P = 0.355$).

412

413 *Annual estimates of carbon losses from soils*

414 Soil carbon losses on a 15 days basis were significantly predicted by a GAMM including
 415 grassland degradation as a fixed factor, and accumulated rainfall during the three previous
 416 months and average soil temperature as fixed covariates nested within degraded and
 417 natural grasslands (likelihood ratio test: $\text{Chi}^2 = 142.6$, $\text{df} = 13$, $P \ll 0.001$, $R^2=65.3\%$;
 418 Table 3). A model including the accumulated rainfall during the three previous months was
 419 considerably better ($\text{AICc} = 768.6$) than one including the average soil water content for
 420 the fortnight ($\text{AICc} = 793.5$; see Supplementary material S5). Accumulated rainfall during
 421 the three previous months positively and significantly influenced soil carbon losses at both
 422 sites, with a steeper slope in the degraded grassland (Figure 6). Soil carbon loss was also
 423 significantly affected in a quadratic-like manner by average soil temperature, particularly
 424 in the natural grassland. Soil carbon losses were higher in the natural than in the degraded
 425 grassland at average fortnight temperatures that maximise soil CO₂ efflux rates (i.e.,
 426 around 20-23 °C), and lower at temperatures above 30 °C.

427 Differences among sites were highly significant ($P = <0.001$), with soil carbon fluxes
 428 larger in the natural (adjusted mean: $9.9 \text{ g C m}^{-2} \text{ 15 days}^{-1}$) than in the degraded (7.2 g C m^{-2}
 429 15 days^{-1}) grassland. The total soil carbon loss per year in 2008 and 2009, when we
 430 sampled the whole annual cycle, ranged between $228.7\text{-}239.1 \text{ g C m}^{-2} \text{ year}^{-1}$ in the natural
 431 and $146.2\text{-}173.6 \text{ g C m}^{-2} \text{ year}^{-1}$ in degraded grasslands (see Table 1). The very different

432 total rainfall in these two years (32.2% lower in 2008 than in 2009; Table 1) contrasts with
433 the very similar total carbon loss estimated (higher in the driest year 2009 than in 2008:
434 4.5% higher in the natural and 18.7% in the degraded grassland), in spite of the above-
435 mentioned positive relationship between carbon loss and accumulated rainfall during the
436 last three months. This counterintuitive result can be easily explained considering the
437 seasonal rainfall pattern in both years: 42.5% of annual rainfall in the driest year 2009
438 occurred in spring (70.5 mm) while this amount was 19.7% (48.2 mm) in 2008.

439 Repeating the previous GAMM separately for the two study sites, 67.8% of variance in
440 soil carbon loss was explained by soil temperature and accumulated rainfall over the last
441 three months in the natural grassland, and 57.2% in the degraded grassland. The exclusive
442 partial effect of soil temperature was larger in the natural (36.3%) than in the degraded
443 grassland (13.8%), while relatively similar amounts of variance were observed for rainfall
444 (16.7% in natural and 22.6% in the degraded grassland).

445

446 **Discussion**

447 *Factors controlling the temporal dynamics of soil CO₂ efflux in dry semiarid grasslands:*

448 *Impact of land degradation*

449 Our study showed that in these dry grassland ecosystems the seasonal pattern of soil CO₂
450 efflux followed mostly environmental variables, but its temporal variability was much
451 larger than changes in soil moisture and soil temperature alone, suggesting that other
452 factors modulate this flux. The observed values are lower than in mesic ecosystems and
453 similar to those reported in other similar ecosystems (e.g. Chen et al. 2008; Zhao et al.
454 2014; Arredondo et al. 2018). Overall, soil CO₂ efflux rates were consistently larger in the
455 natural than in the degraded grassland, mostly as a result of larger vegetation cover and
456 plant activity and consequently, soil activity (Rey et al. 2012). Indeed, soil moisture was

457 the main controlling factor of soil CO₂ efflux in the degraded site (25.4%) whereas the
458 combined effect of soil moisture, soil temperature and seasonality, was the main driver in
459 the natural grassland (27.5% of variation accounted for). The strong combined effect of
460 soil temperature and soil moisture on soil CO₂ efflux has already been observed in similar
461 semiarid ecosystems (i.e. Arredondo et al. 2018; Barron-Gafford et al. 2011; Liu et al.
462 2018).

463 At both sites, soil CO₂ efflux responded positively to soil moisture values up to ca. 20%
464 and then remained practically constant or even decreased. Similar or even lower threshold
465 values have been observed in other semiarid grasslands (e.g. Oyonarte et al. 2012;
466 Arredondo et al. 2018). Above this soil moisture value, soil CO₂ efflux rates were larger in
467 the degraded than in the natural grassland. Thus, soil biological activity in the degraded
468 grassland was much more limited by water availability than in the natural site which agrees
469 with previous studies at these sites (Rey et al. 2011). Greater sensitivity of biological
470 activity to soil moisture in drier sites has been observed elsewhere (Averill et al. 2016).
471 Soil microbes may adapt to dry conditions and water pulses in several ways. Local
472 variation in the response of microbes to soil moisture may include legacy effects (Hawkes
473 & Keitt 2015), adaptation or microbial species to rainfall regime optimising enzyme
474 production (Collins et al. 2008; Hawkes et al. 2011), and persistence of enzymes in
475 drought periods allowing for accumulation of soluble substrates that are available upon
476 rewetting (Manzoni et al. 2012). This is supported by manipulative studies where rainfall is
477 reduced showing that soil enzyme activities are more sensitive to changes in soil moisture
478 (Alster et al. 2013).

479 In agreement with previous studies (e.g. Cable et al. 2008), this study found that a
480 significant amount of variation in soil CO₂ efflux can be attributed to unknown temporal
481 effects (between 44 and 52%). In order to explain other factors controlling the temporal

482 variability in soil CO₂ efflux, we showed that the inclusion of seasonality as a proxy of
483 plant activity and soil water effects into a model significantly improved explained
484 variance. Recent studies have included day of the year as a predictor to model soil CO₂
485 efflux (Acosta et al. 2018). The importance of incorporating other factors into models have
486 been highlighted by recent studies showing the potential importance of photosynthetic
487 carbon inputs for understanding the magnitude of soil CO₂ efflux (Vargas et al. 2011) or
488 even microbial activity and community composition (Liu et al. 2018). Thus, this study
489 supports that plant productivity is an important factor controlling soil CO₂ effluxes that
490 should be taken into account in order to accurately predict the temporal variability of this
491 flux in these semiarid grasslands (Roby et al. 2019). Consequently, the loss of plant cover
492 resulting from land degradation will affect soil carbon losses.

493

494 *Spatial variability in soil CO₂ efflux*

495 We aimed to characterise the large spatial variability in soil CO₂ efflux typical of these dry
496 ecosystems by analysing the response of different soil covers to environmental variables.
497 Since soil carbon and soil microclimate differed among soil covers, we expected different
498 contributions to soil carbon losses. Although small, differences between soil CO₂ efflux
499 rates among soil covers were highly significant. Vegetation cover alters soil properties not
500 only by reducing solar radiation (Zou et al. 2007), but also by increasing root density, soil
501 nutrients and soil organic matter (Jackson et al. 2000). This results in changes in soil
502 structure underneath plants with fine-textured soils that have high water-holding capacity
503 (Jobbagy & Jackson, 2000), increasing the availability of water in surface layers where
504 most microbes are found (Rey et al. 2008). Thus, changes in soil structure as a result of
505 plant cover may have also contributed to the observed differences in the spatial variation in

506 soil CO₂ efflux, but we expect that the contribution was small given that most roots are
507 also found underneath plants (Rey et al. 2011).

508 Our statistical approach allowed us to compare soil CO₂ efflux rates removing the different
509 environmental conditions under vegetated areas, biological soil crusts and bare soil. The
510 analysis revealed that soil CO₂ efflux rates differed between soil covers beyond
511 environmental conditions, with highest rates under biological soil crusts at both sites and
512 lowest under bare soil which agrees with previous studies (Li et al. 2018). Some of the
513 observed differences were caused by higher soil organic matter concentration underneath
514 plants (Leon et al. 2014; Rey et al. 2017) so that when we expressed soil carbon fluxes on
515 a carbon basis, differences between soil covers and sites differed from soil CO₂ efflux rates
516 on an area basis. Soil CO₂ efflux rates measured under vegetated areas were lowest while
517 larger amounts of soil carbon losses were measured under bare soil. These results indicate
518 that for the same environmental conditions, and despite higher soil organic matter and
519 carbon concentrations under plants, a larger proportion of carbon is lost from bare soils
520 compared with soils under vegetated areas. Since heterotrophic respiration is more
521 sensitive to changes in soil moisture than autotrophic respiration (Carbone et al. 2008),
522 higher sensitivity to soil moisture under bare soils can be expected. However, in a previous
523 study, Rey et al. (2017) found that substrate availability limits the response of soil CO₂
524 efflux from bare soils to larger rainfall events, so soils under biological soil crusts lost
525 more carbon than the other two soil covers.

526 In a previous study investigating the immediate response of soil CO₂ efflux to rainfall
527 amount and timing at the same study sites, Rey et al. (2017) showed that soils covered by
528 biological soil crust were most responsive to precipitation, responding even to small
529 rainfall events, more than vegetated and bare soil patches. This agrees with other studies
530 showing that biological soil crusts respond more than plants and microbes to small rainfall

531 events (i.e. Cable & Huxman 2004; Bowling et al. 2011; Rey et al. 2017). Soil moisture at
532 3.5 cm may not reflect small changes in surface moisture capable of activating biological
533 soil crusts communities as recently shown (Tucker et al. 2017). Indeed, previous studies
534 have shown that biocrusts gain similar amounts of water as vascular plants (Zhang et al.
535 2008; Berdugo et al. 2014). In this study, soils covered by biological soil crusts respired
536 more than vegetated and bare soils over the study years, which agrees with previous
537 studies in similar areas (Castillo-Monroy et al. 2011; Ouyang & Hu 2017; Tucker et al.
538 2017; Li et al. 2018). Besides changes in soil physical conditions, changes in microbial
539 communities and soil carbon and nitrogen substrates underneath biological soil crusts
540 could also explain higher soil carbon fluxes (Zhao et al. 2014; Fisher et al. 2020).
541 However, biological soil crusts get activated by small precipitation events and high relative
542 humidity favoring CO₂ uptake as previously observed at the same site (Rey et al. 2012)
543 and in other studies (Tucker et al. 2017; Li et al. 2018). The net carbon balance of these
544 soils covered by biological soil crusts are beyond the scope of this study. Since most of the
545 rainfall events were small (between 47 and 70% of less than 5 mm), soils covered by
546 biological soil crusts also contributed the most to soil carbon losses in these ecosystems.
547 Thus, as suggested in this study, changes in precipitation patterns may alter the respiratory
548 contribution from different components of the ecosystem, thereby altering the carbon
549 budget of dryland ecosystems (Li et al. 2018).

550

551 *Impact of precipitation on soil carbon fluxes*

552 Precipitation in this semiarid area is very low (averaging 200 mm) falling in few events
553 (around 10% of the days) and is characterised by large temporal variability. Over the study
554 years, rainfall ranged from 165 mm in 2009 to 364 mm in 2010, so the study period
555 covered dry, intermediate and wet years. Although only 10% of the events were larger than

556 15 mm, they constituted between 36 and 52% of total annual precipitation. Thus, most rain
557 occurs in few extreme events in the year as it is often the case in drylands (Knapp et al.
558 2015). Apart from consistent dry summers, timing was highly variable with rainfall falling
559 in autumn, spring and winter. Precipitation was a much better factor explaining seasonal
560 soil carbon fluxes than soil moisture. In particular, we found that cumulative rainfall over
561 three months was the best predictor of soil carbon losses over two weeks. The effect of
562 precipitation was larger for the degraded grassland, particularly for accumulated rainfall
563 larger than 60 mm, suggesting that degraded ecosystems are more strongly limited by soil
564 moisture. This agrees with other studies (Liu et al. 2016), suggesting that ecosystem
565 sensitivity to precipitation increases with aridity. As previously observed (Arredondo et al.
566 2018), plants dampened the sensitivity to moisture while increasing the sensitivity to
567 temperature. Our study supports these findings as the natural grassland was less responsive
568 to precipitation and more sensitive to temperature than the degraded one with much less
569 vegetation cover. As highlighted by Knapp et al. (2015) and Liu et al. (2016), experiments
570 should therefore focus on manipulating not only the amount of rain but the timing and
571 number of extreme events, as timing seems to be more important for soil biological activity
572 than rainfall amount.

573 Maximum soil CO₂ efflux rates also coincide with the peak of maximum photosynthesis in
574 spring for Mediterranean ecosystems (Jarvis et al. 2007) with adequate microclimatic
575 conditions for soil microbial decomposition. In agreement with previous studies
576 (Robertson et al. 2009; Bell et al. 2014; Averill et al. 2016), this study supports that soil
577 biological activity can be more responsive to seasonal availability of precipitation than to
578 the amount of annual precipitation. Indeed, the highest soil carbon losses were estimated in
579 the driest year (2009) and the lowest in the wettest with almost doubled the amount of
580 rainfall (2010). The main difference between these years was the timing of the events that

581 mostly occurred in the moments of maximum plant and biocrust activity with optimum
582 temperatures in spring in the driest year.

583 This study also highlights the important interaction between precipitation and land
584 degradation. Land degradation affects more than 20% of semiarid lands and is expected to
585 increase with climate change (Reed et al. 2012). As a result, plant and soil cover are lost
586 and in turn, biochemical and biophysical processes. The loss of vegetation cover and
587 concomitant productivity reduction alters the ecosystem energy balance, hydrological
588 budget, and productivity (Barron-Gafford et al. 2014; Ghezzehei et al. 2019). Larger
589 interspace patches with rock and bare soil cover, as well as lower soil organic matter
590 content in the degraded site, resulted in larger evaporative losses and lower soil moisture
591 contents than in the natural grassland, and thus, lower soil carbon fluxes for the same
592 precipitation amount, but more sensitive to increases in rainfall amount. This greater
593 sensitivity might be related to comparatively greater extensions of plant interspaces in the
594 degraded grassland, which then translates into greater exposure to radiation, and
595 accelerated cycles of desiccation, higher temperatures, sensible heat fluxes and rewetting.
596 As a consequence, precipitation caused larger carbon fluxes, particularly for intense
597 rainfall events. Previous studies (Fei et al. 2018) have attributed soil carbon losses to
598 changes in soil properties resulting from land degradation.

599 Current models predict rainfall reduction, increased drought periods and increased extreme
600 rainfall events (Groisman et al. 2005; Huntington 2006; IPCC 2014). Expected changes in
601 rainfall patterns will alter soil moisture dynamics, affecting multiple ecosystem processes
602 in drylands (Greve et al. 2014). This study supports that both, changes in rainfall amount
603 and rainfall patterns, will affect belowground activity and soil carbon fluxes, particularly in
604 degraded grasslands. Furthermore, since most of the rain falls in few extreme rainfall
605 events, in agreement with previous work (Fay et al. 2008), this study also suggests that an

606 increase in extreme events will likely lead to further soil carbon losses via soil carbon
607 fluxes, aggravating land degradation.

608 **References**

- 609 Aanderud ZT, Schoolmaster Jr. DR, Lennon JT (2011) Plants mediate the sensitivity of
610 soil respiration to rainfall variability. *Ecosystems* 14:156-167
- 611 Acosta M, Darenova E, Krupkova L, et al. (2018) Seasonal and inter-annual variability of
612 soil CO₂ efflux in a Norway spruce forest over an eight-year study. *Agricultural &*
613 *Forest Meteorology* 256-257: 93-103
- 614 Alekseev A, Alekseeva P, Kalinin M, et al. (2018) Soils response to the land use and soil
615 climatic gradients at ecosystem scale: Mineralogical and geochemical data. *Soil Tillage*
616 *Research* 180: 38-47
- 617 Alster CJ, German DP, Lu Y, et al. (2013) Microbial enzymatic responses to drought and
618 to nitrogen addition in a southern California grassland. *Soil Biology & Biochemistry*
619 64: 68-79
- 620 Ahlström A, Raupach MR, Schurgers G, et al. (2015) The dominant role of semi-arid
621 ecosystems in the trend and variability of the land CO₂ sink. *Science* 348: 895-899
- 622 Arredondo T, Delgado-Balbuena J, Huber-Sannwald E, García-Moya E (2018) Does
623 precipitation affects soil respiration of tropical semiarid grasslands with different plant
624 cover types? *Agriculture, Ecosystems & Environment* 251: 218-225
- 625 Averill C, Waring BG, Hawkes, CV (2016) Historical precipitation predictably alters the
626 shape and magnitude of microbial functional response to soil moisture. *Global Change*
627 *Biology* 22: 1957-1964
- 628 Barron-Gafford GA, Cable JM, Bentley LP, et al. (2014) Quantifying the timescales over
629 which exogenous and endogenous conditions affect soil respiration. *New Phytologist*
630 202: 442-454
- 631 Barron-Gafford GA, Scott RL, Jenerette DG, Huxman TE (2011) The relative controls of
632 temperature, soil moisture, and plant functional group on soil CO₂ efflux at diel,
633 seasonal and annual scales. *Journal of Geophysical Research* 116: G01023
- 634 Bell CW, Tissue DT, Loik ME, et al. (2014) Soil microbial and nutrient responses to seven
635 years of seasonally altered precipitation in a Chihuahuan Desert grassland. *Global*
636 *Change Biology* 20: 1657-1673
- 637 Belnap J, Lange OL (2003) *Biological soil crusts: structure, function, and management.*
638 Springer, Berlin
- 639 Berdugo M, Soliveres S, Maestre FT (2014) Vascular plants and biocrusts modulate how
640 abiotic factors affect wetting and drying events in drylands. *Ecosystems* 17: 1242-1256
- 641 Bond-Lamberty B, Thomson A (2010) A global database of soil respiration data.
642 *Biogeoscience Discussion* 7: 1915-1926
- 643 Borken W, Matzner E (2009) Reappraisal of drying and wetting effects on C and N
644 mineralization and fluxes in soils. *Global Change Biology* 15: 808-824
- 645 Bowling D, Grote E, Belnap J (2011) Rain pulse response of soil CO₂ exchange by
646 biological soil crusts and grasslands of the semiarid Colorado Plateau United States.
647 *Journal of Geophysical Research* 116: G03028
- 648 Burke IC, Mosier AR, Hook PB, et al. (2008) Soil organic matter and nutrient dynamics of
649 shortgrass steppe ecosystems. In: Lauenroth WK, Burke IC (eds) *Ecology of the*
650 *shortgrass steppe.* Oxford University Press, New York, pp 306-341

- 651 Cable JM, Huxman TE (2004) Precipitation pulse size effects on Sonoran Desert soil
652 microbial crusts. *Oecologia*, 141: 317-324
- 653 Cable JM, Ogle K, Williams DG, et al. (2008) Soil texture drives responses of soil
654 respiration to precipitation pulses in the Sonoran Desert: implications for climate
655 change. *Ecosystems* 11: 961-979
- 656 Cammeraat LH (1996) The MEDALUS Core Field Programme: An Overview of sites and
657 Methodology. In: Brandt CJ, Thornes JB (eds) *Mediterranean Desertification and Land*
658 *Use*. John Wiley & Sons Ltd, Chichester, pp 87-110
- 659 Carbone MS, Winston GC, Trumbore SE. (2008) Soil respiration in perennial grass and
660 shrub ecosystems: linking environmental controls with plant and microbial sources on
661 seasonal and diel timescales. *Journal of Geophysical Research* 113: G02022
- 662 Castillo-Monroy AP, Maestre FT, Rey A, et al. (2011) Biological soil crust microsites are
663 the main contributor to soil respiration in a semiarid ecosystem. *Ecosystems* 14: 835-
664 847
- 665 Chen S, Lin G, Huang J, et al. (2008) Responses of soil respiration to simulated
666 precipitation pulses in semiarid steppe under different grazing regimes. *Journal of Plant*
667 *Ecology* 4: 237-248
- 668 CMA (1999) Delimitación de las unidades geomorfoedáficas del Parque Natural Cabo de
669 Gata - Níjar. Bases de datos de la Consejería Medio Ambiente, Junta de Andalucía.
- 670 Collins SL, Sinsabaugh RL, Crenshaw C, et al. (2008) Pulse dynamics and microbial
671 processes in aridland ecosystems: pulse dynamics in aridland soils. *Journal of Ecology*
672 96: 413-420
- 673 Correia AC, Minunno F, Caldeira MC, et al. (2012) Soil water availability strongly
674 modulates soil CO₂ efflux in different Mediterranean ecosystems: Model calibration
675 using the Bayesian approach. *Agriculture, Ecosystems & Environment* 161: 88-100
- 676 Dregne HE (2002) Land degradation in drylands. *Arid Research & Management* 16:99-132
- 677 Escribano P (2002) Definition of zonation units in Cabo de Gata-Níjar Natural Park.
678 Thesis Report GIRS-2002-045. Wageningen University, Wageningen
- 679 Fay PA (2009) Precipitation variability and primary productivity in water-limited
680 ecosystems: how plants ‘leverage’ precipitation to ‘finance’ growth. *New Phytologist*
681 181: 5-8
- 682 Fay PA, Kauffman DM, Nipper JP, et al. (2008) Changes in grassland ecosystem function
683 due to extreme rainfall events: implications for responses to climate change. *Global*
684 *Change Biology* 14: 1600-1608
- 685 Fei P, Xian X, Quangang Y, et al. (2018) Changes of soil properties regulate the soil
686 organic carbon loss with grassland degradation on the Qinghai-Tibet Plateau.
687 *Ecological Indicators* 93: 572-580
- 688 Feng S, Fu Q (2013) Expansion of global drylands under a warming climate. *Atmospheric*
689 *Chemistry & Physics* 13: 14637-14665
- 690 Fisher K, Jefferson JS, Vaishampayan P (2020) Bacterial Communities of Mojave Desert
691 Biological Soil Crusts Are Shaped by Dominant Photoautotrophs and the Presence of
692 Hypolithic Niches. *Frontiers in Ecology & Evolution*, 21: doi.10.3389/2019.00518

- 693 Ghezzehei TA, Sulman B, Arnold CL et al. (2019) On the role of soil water retention
694 characteristic on aerobic microbial respiration. *Biogeosciences* 16: 1187–1209
- 695 Greve P, Orlowsky B, Mueller B, et al. (2014) Global assessment of trends in wetting and
696 drying over land *Nature Geoscience* 7: 716–21
- 697 Groisman PY, Knight RW, Easterling DR, et al. (2005) Trends in intense precipitation in
698 the climate record. *Journal of Climate* 18: 1326-1350
- 699 Hawkes CV, Keitt TH (2015) Resilience vs. historical contingency in microbial responses
700 to environmental change (eds. Classen A). *Ecology Letters* 18: 612-625
- 701 Hawkes CV, Kivlin SN, Rocca JD, et al. (2011) Fungal community responses to
702 precipitation. *Global Change Biology* 17: 1637-1645
- 703 Huang N, Wang L, Song XP, et al. (2020) Spatial and temporal variations in global soil
704 respiration and their relationships with climate and land cover. *Science Advances* 6:
705 eabb8508
- 706 Huntington TG (2006) Evidence for intensification of the global water cycle: Review and
707 synthesis. *Journal of Hydrology* 319: 83-95
- 708 IPCC (2014) Fourth Assessment Report of the Intergovernmental Panel on Climate
709 Change
- 710 Jackson RB, Schenk HJ, Jobaggy EG, et al. (2000) Belowground consequences of
711 vegetation change and their treatment in models. *Ecological Applications* 10: 470-483
- 712 Jarvis PG, Rey A, Petsikos C, et al. (2007) Drying and wetting of soils stimulates
713 decomposition and carbon dioxide emission: the “Birch Effect”. *Tree Physiology* 27:
714 929-940
- 715 Jobbagy EG, Jackson RB. (2000) The vertical distribution of soil organic carbon and its
716 relation to climate and vegetation. *Ecological Applications* 10: 423-436
- 717 Knapp AK, Beier C, Briske DD, et al. (2008) Consequences of more extreme precipitation
718 regimes for terrestrial ecosystems. *Biosciences* 58: 811-821
- 719 Knapp AK, Hoover DL, Wilcox KR, et al. (2015) Characterizing differences in
720 precipitation regimes of extreme wet and dry years: implications for climate change
721 experiments. *Global Change Biology* 21: 2624-2633
- 722 Legendre P, Legendre L (1998) *Numerical Ecology*, 2nd English ed. Elsevier, Amsterdam
- 723 Leon E, Vargas R, Bullock S, et al. (2014) Hot spots, hot moments, and spatio-temporal
724 controls on soil CO₂ efflux in a water-limited ecosystem. *Soil Biology & Biochemistry*
725 77: 12-21
- 726 Li XJ, Zhao Y, Yang HT, et al. (2018) Soil respiration of biologically-crusted soils in
727 response to simulated precipitation pulses in the Tegger Desert, northern China.
728 *Pedosphere* 28: 103-113
- 729 Liu T, Wang L, Zhang J, et al. (2018) Comparing soil carbon loss through respiration and
730 leaching under extreme precipitation events in arid and semiarid grasslands.
731 *Biogeosciences* 15: 1627-1641
- 732 Liu L, Wang X, Lajeunesse MJ, et al. (2016) A cross-biome synthesis of soil respiration
733 and its determinants under simulated precipitation changes. *Global Change Biology* 22:
734 1394-1405

- 735 Liu Y, Zhao C, Shang Q, et al. (2019) Responses of soil respiration to spring drought and
736 precipitation pulse in a temperate oak forest. *Agricultural & Forest Meteorology* 268:
737 289-298
- 738 Liu YR, Delgado-Vaquerizo M, Wang JT, et al. (2018) New insights into the role of
739 microbial community composition in driving soil respiration rates. *Soil, Biology &
740 Biochemistry* 118: 35-41
- 741 López-Ballesteros A, Serrano-Ortiz P, Sánchez-Cañete EP, et al. (2015) Enhancement of
742 the net CO₂ release of a semiarid grassland in SE Spain by rain pulses. *Journal of
743 Geophysical Research: Biogeosciences* 121, doi:10.1002/2015JG003091 □
- 744 Maestre FT, Escolar C, Ladrón de Guevara M, et al. (2013) Changes in biocrust cover
745 drive carbon cycle responses to climate change in drylands. *Global Change Biology* 19:
746 3835-3847
- 747 Manzoni S, Chakrawal A, Fischer T, et al. (2020) Rainfall intensification increases the
748 contribution of rewetting pulses to soil respiration. *Biogeosciences*
749 <https://doi.org/10.5194/bg-2020-95>
- 750 Manzoni S, Schimel JP, Porporato A (2012) Responses of soil microbial communities to
751 water stress: results from a meta-analysis. *Ecology* 93: 930-938
- 752 Mitra B, Miao G, Minick K, et al (2019) Disentangling the effects of temperature,
753 moisture, and substrate availability on soil CO₂ efflux. *Journal of Geophysical Research*
754 124: 2060–2075
- 755 Nielsen UN, Ball BA (2015) Impacts of altered precipitation regimes on soil communities
756 and biogeochemistry in arid and semi-arid ecosystems. *Global Change Biology* 21:
757 1407-1421
- 758 Ouyang H, Hu C (2017) Insight into climate change from the carbon exchange of biocrusts
759 utilizing non-rainfall water. *Scientific Reports* 7: 2573
- 760 Oyonarte C, Rey A, Raimundo J, et al. (2012) The use of soil respiration as an ecological
761 indicator in arid ecosystems of the SE of Spain: Spatial variability and controlling
762 factors. *Ecological Indicators* 14: 40-49
- 763 R Core Team (2018) R: A language and environment for statistical computing. R
764 Foundation for Statistical Computing, Vienna, Austria. <http://www.R-project.org/>
- 765 Reed, SC, Coe, KK, Sparks, JP, et al. (2012) Changes to dryland rainfall result in rapid
766 moss mortality and altered soil fertility. *Nature Climate Change* 2: 752–755
- 767 Rey A, Oyonarte C, Moran T, et al. (2017) Changes in soil moisture predict soil carbon
768 losses upon rewetting in a perennial semiarid steppe in SE Spain. *Geoderma* 287: 135-
769 146
- 770 Rey A (2015) Mind the gap: non-biological processes contributing to soil CO₂ efflux.
771 *Global Change Biology* 21, 1752-1761.
- 772 Rey A, Belelli-Marchesini L, Were A, et al. (2012) Wind as the main driver of net
773 ecosystem carbon balance of a semiarid steppe ecosystem in the SE of Spain. *Global
774 Change Biology* 18: 539-554
- 775 Rey A, Pegoraro E, Oyonarte C, et al. (2011) Impact of land degradation on soil respiration
776 in a steppe (*Stipa tenacissima* L.) semi-arid ecosystem in the SE of Spain. *Soil Biology
777 & Biochemistry* 43: 393-403

- 778 Rey A, Pegoraro E, Jarvis PG (2008) Carbon mineralization rates at different soil depths
779 across a network of European forest sites (FORCAST). *European Journal of Soil*
780 *Science* 59: 1049-1062
- 781 Reichstein M, Beer C (2008) Soil respiration across scales: The importance of a model–
782 data integration framework for data interpretation. *Journal Plant Nutrition Soil Science*
783 171: 344-354
- 784 Robertson TR, Bell CW, Zak JC, et al. (2009) Precipitation timing and magnitude
785 differentially affect aboveground annual net primary productivity in three perennial
786 species in a Chihuahuan Desert grassland. *New Phytologist* 181: 230-242
- 787 Roby MC, Scott, RL, Moore Ross DJP et al. (2019) Environmental and vegetative controls
788 on soil CO₂ efflux in three semiarid ecosystems. *Soil Systems* 3, 6
- 789 Scharlemann JPW, Tanner EVJ, Hiederer R, et al. (2014) Global soil carbon:
790 understanding and managing the largest terrestrial carbon pool. *Carbon Management* 5:
791 81-91
- 792 Schimel DS (2010) Climate. Drylands in the Earth system. *Science* 327: 418-419
- 793 Sitch S, Huntingford C, Gedne N, et al. (2008) Evaluation of the terrestrial carbon cycle,
794 future plant geography and climate-carbon cycle feedbacks using five dynamic global
795 vegetation models (DGVMs). *Global Change Biology* 14: 2015-2039
- 796 Smith MD (2011) The ecological role of climate extremes: current understanding and
797 future prospects. *Journal of Ecology* 99: 651-655
- 798 Thomas AD, Elliott DR, Dougill AJ, et al. (2018) The influence of trees, shrubs, and
799 grasses on microclimate, soil carbon, nitrogen, and CO₂ efflux: Potential implications of
800 shrub encroachment for Kalahari rangelands. *Land Degradation Development* 29: 1306-
801 1316
- 802 Tucker CL, McHugh TA, Howell A, et al. (2017) The concurrent use of novel soil surface
803 microclimate measurements to evaluate CO₂ pulses in biocrusted interspaces in a cool
804 desert ecosystem. *Biogeochemistry* 135: 239-249
- 805 Vargas R, Carbone MS, Reichstein M, et al. (2011) Frontiers and challenges in soil
806 respiration research: from measurements to model-data integration. *Biogeochemistry*
807 102: 1-13
- 808 Wood SN (2006) *Generalized Additive Models: An Introduction with R*. Chapman and
809 Hall/CRC Press, Boca Raton
- 810 Wood SN (2017) Package ‘mgcv’. Version 1.8-17. Downloadable from [https://cran.r-](https://cran.r-project.org/web/packages/mgcv/mgcv.pdf)
811 [project.org/web/packages/mgcv/mgcv.pdf](https://cran.r-project.org/web/packages/mgcv/mgcv.pdf).
- 812 WRB (2006) World Reference Base for Soil Resources 2006. *World Soil Resources*
813 Reports No 103. FAO, Rome, 128 pp.
- 814 Zar JH (1999) *Biostatistical Analysis*. 4.^a ed. Prentice Hall, Upper Saddle River, NJ, USA
- 815 Zhang R, Xhao X, Zuo X (2019) Effect of manipulated precipitation during the growing
816 season on soil respiration in the desert-grasslands in Inner Mongolia, China. *Catena*
817 176: 73-80.
- 818 Zhang LH, Chen YN, Zhao RF, et al. (2010) Significance of temperature and soil water
819 content on soil respiration in three desert ecosystems in Northwest China. *Journal of*
820 *Arid Environments* 74: 1200-1211

- 821 Zhang ZS, Liu LC, Li XR et al. (2008) Evaporation properties of a revegetated area of the
822 Tengger Desert, North China. *Journal of Arid Environments* 72: 964-973
- 823 Zhao J, Li R, Li X, et al. (2017) Environmental controls on soil respiration in alpine
824 meadow along a large altitudinal gradient on the central Tibetan Plateau. *Catena* 159:
825 84-92
- 826 Zhao Y, Li X, Zhang Z, et al (2014) Biological soil crusts influence carbon release
827 responses following rainfall in a temperate desert, northern China. *Ecological Research*
828 29: 889-896
- 829 Zou CB, Barron-Gafford GA, Breshears DD (2007) Effects of topography and woody
830 plant canopy cover on near-ground solar radiation, Relevant energy inputs for
831 ecohydrology and hydrogeology. *Geophysical Research Letters* 34: L24S21
- 832

833
834

Figure legends

835 **Figure 1**

836 Seasonal variability in: (a) soil temperature ($^{\circ}\text{C}$) and (b) soil volumetric water content (%)
837 measured at 3.5 cm depth, (c) mean (for the three soil covers) soil CO_2 efflux rates (μmol
838 $\text{CO}_2 \text{ m}^{-2} \text{ s}^{-1}$) for each site (natural and degraded grasslands), and (d) precipitation (mm)
839 spanning the study period (January 2007-July 2010). Symbols represent the mean \pm 1SE (n
840 = 6 soil covers).

841

842 **Figure 2**

843 Conceptual model with variance partitioning of the factors controlling soil CO_2 efflux
844 ($\mu\text{mol m}^{-2} \text{ s}^{-1}$) at both sites (natural –upper figures– and degraded –lower figures–
845 grasslands): *soil temperature* ($^{\circ}\text{C}$), *soil water content* (%) and *seasonality*. The *Combined*
846 *Effect* refers to the shared variance among predictors, as opposed to their partial exclusive
847 effects.

848

849 **Figure 3**

850 Partial residual plots of: (a) *soil temperature* ($^{\circ}\text{C}$), (b) *soil water content* (%) and (c)
851 *seasonality* on soil CO_2 efflux ($\mu\text{mol CO}_2 \text{ m}^{-2} \text{ s}^{-1}$). Shaded areas represent 95% confidence
852 intervals.

853

854 **Figure 4**

855 Modelled response of soil CO_2 efflux ($\mu\text{mol CO}_2 \text{ m}^{-2} \text{ s}^{-1}$) to soil temperature ($^{\circ}\text{C}$) and soil
856 moisture (%) in the natural (a) and degraded (b) grasslands.

857

858

859 **Figure 5**

860 Soil CO₂ efflux values expressed as: (a) measured mean values ($\mu\text{mol m}^{-2} \text{s}^{-1}$), (b) adjusted
861 means ($\mu\text{mol m}^{-2} \text{s}^{-1}$) and (c) mean soil carbon loss ($\text{mg C g C}^{-1} \text{day}^{-1}$) for each soil cover:
862 under plant cover (VEG), biological soil crust (BSC) and bare soil (BS) in each site:
863 natural and degraded grassland over the entire study period (January 2007-July 2010). Bars
864 represent the mean ($\pm 1\text{SE}$, $n = 6$ replicates per soil cover) for the whole duration of the
865 study (90 measured days). Bars with different letters are significantly different ($P < 0.05$)
866 between soil covers within sites (post hoc test).

867

868 **Figure 6**

869 Partial residual plots: (a) *rainfall amount* (accumulated over the last three months) (mm)
870 and (b) *soil temperature* ($^{\circ}\text{C}$) (mean over the fortnight) on soil carbon losses ($\text{g C m}^{-2} 15$
871 days^{-1}) in the natural and degraded grasslands. The range of soil temperature is restricted to
872 the natural variation measured at each study area. Shaded areas represent 95% confidence
873 intervals.

874

Figure 1

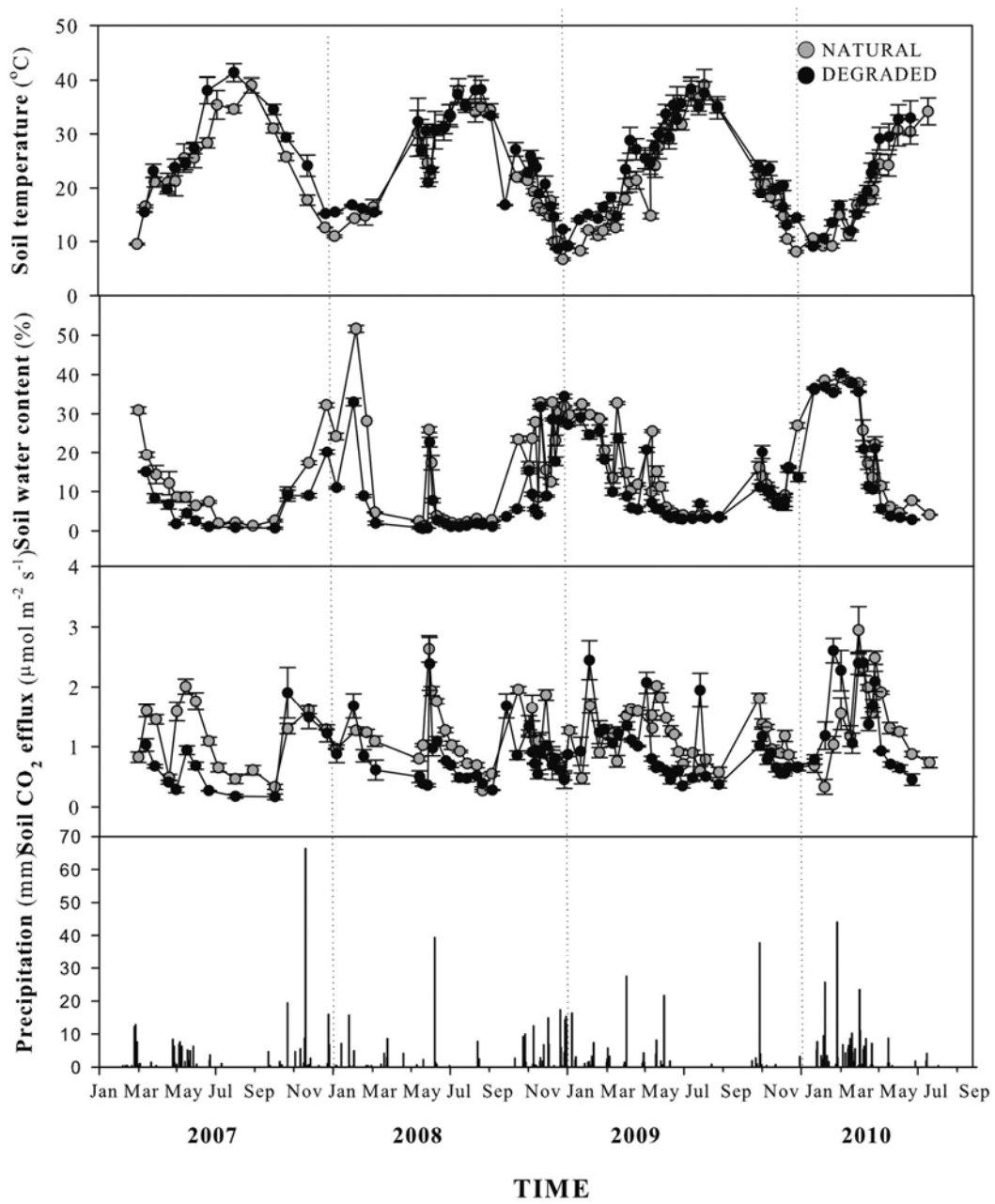


Figure 2

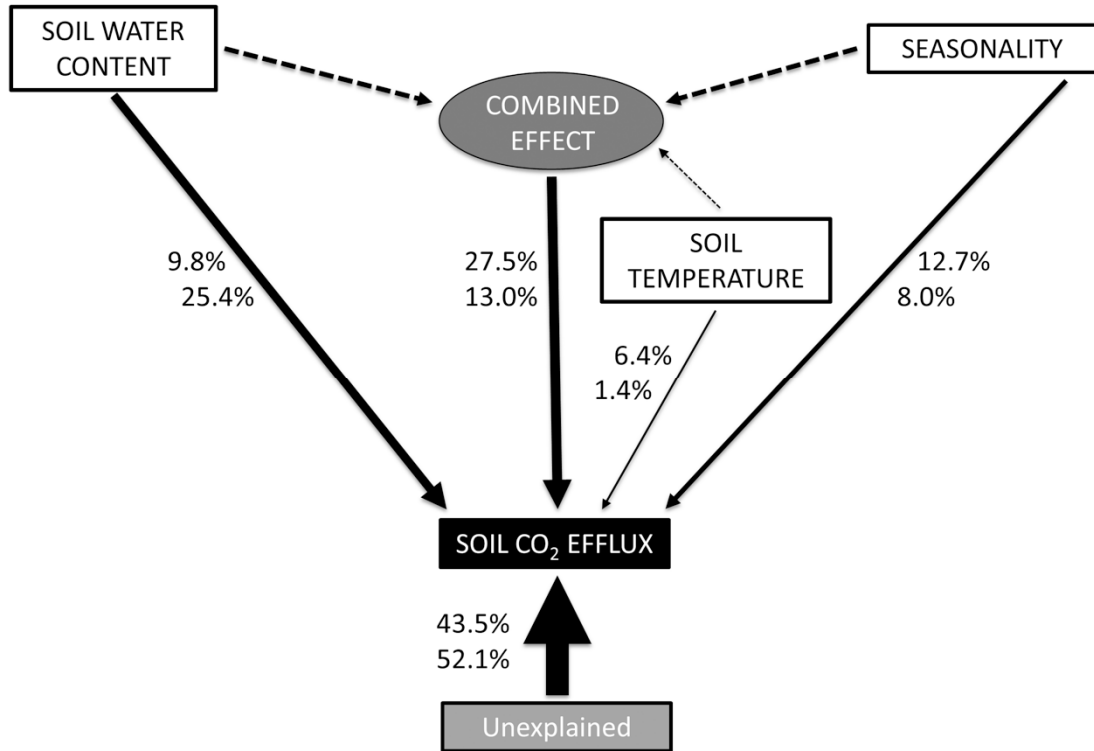


Figure 3

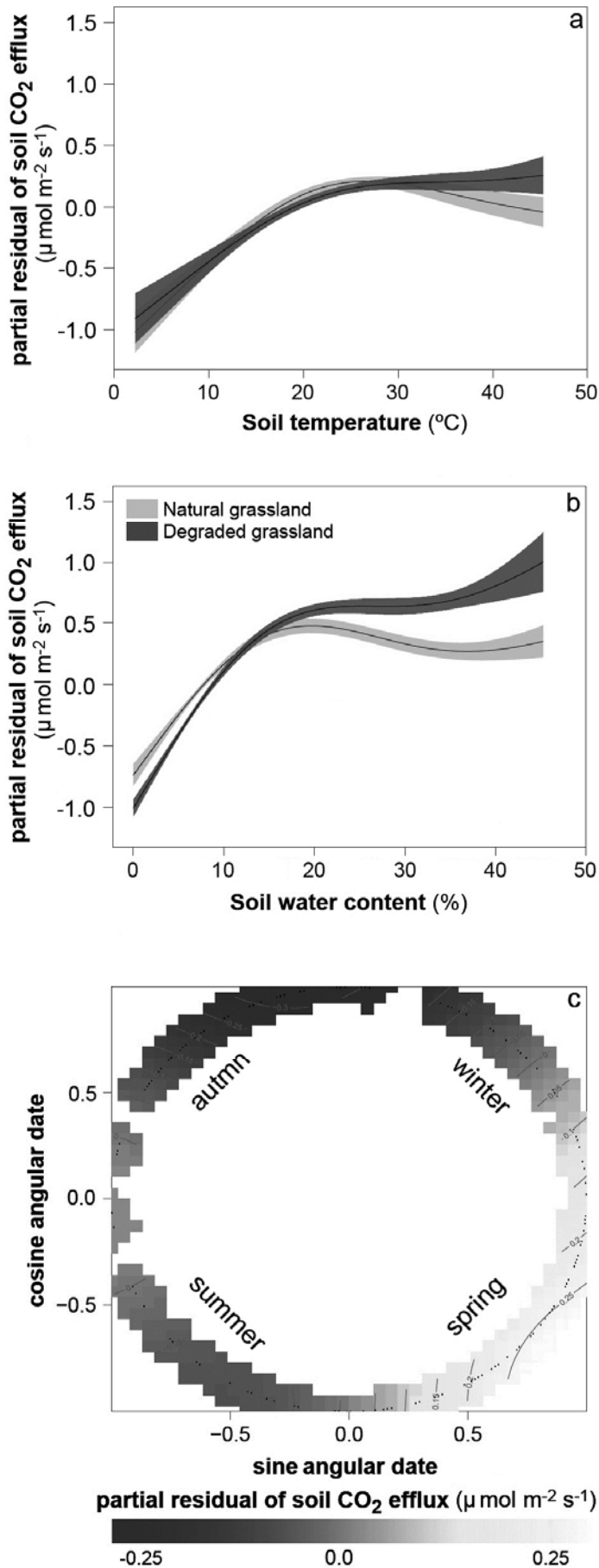


Figure 4

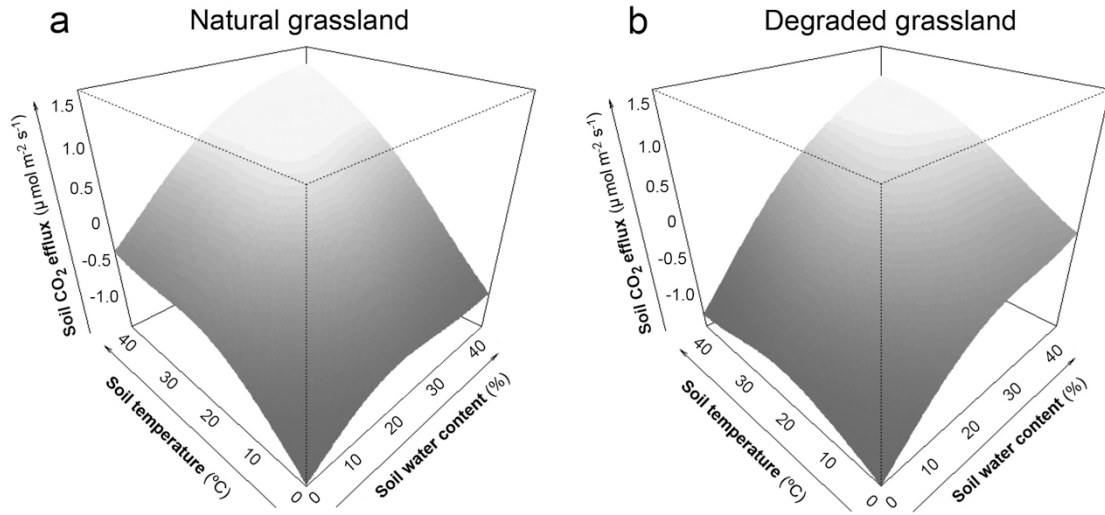


Figure 5

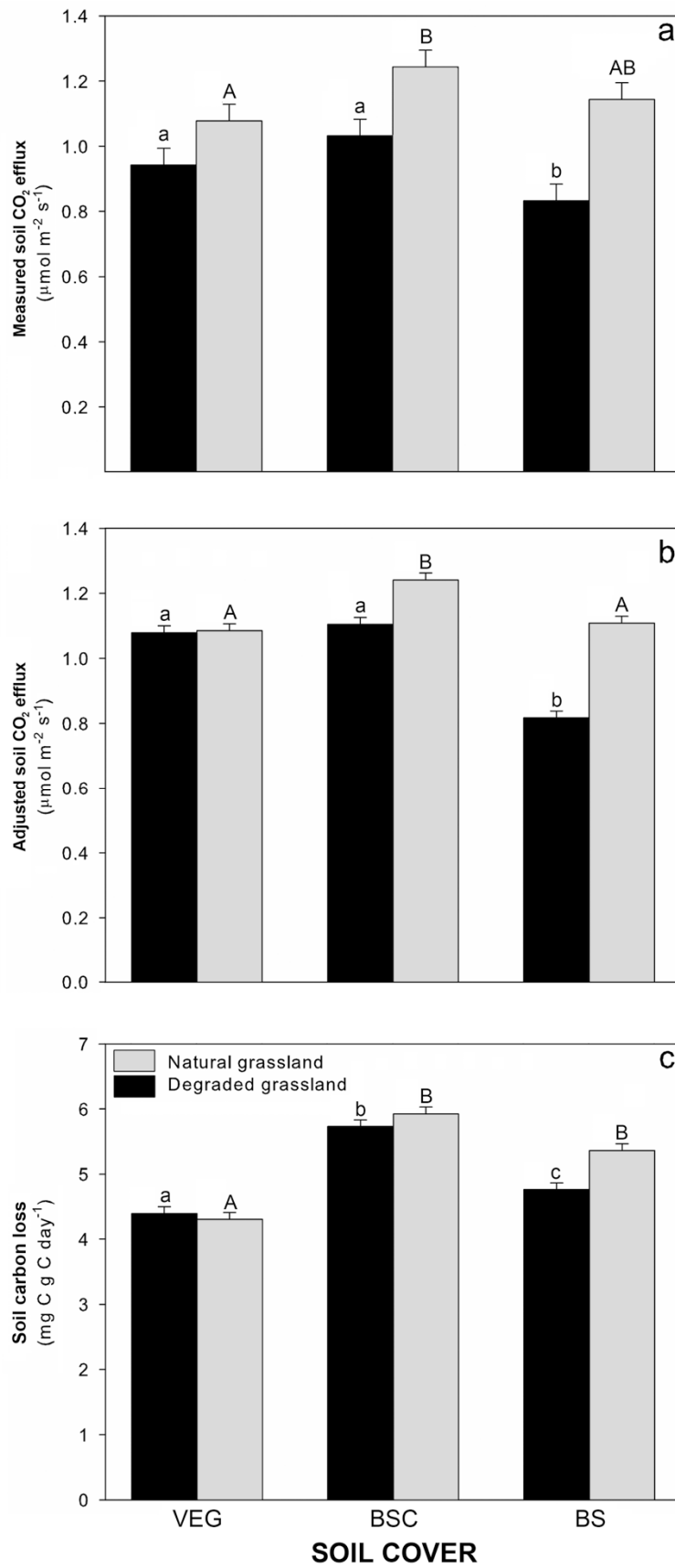


Figure 6

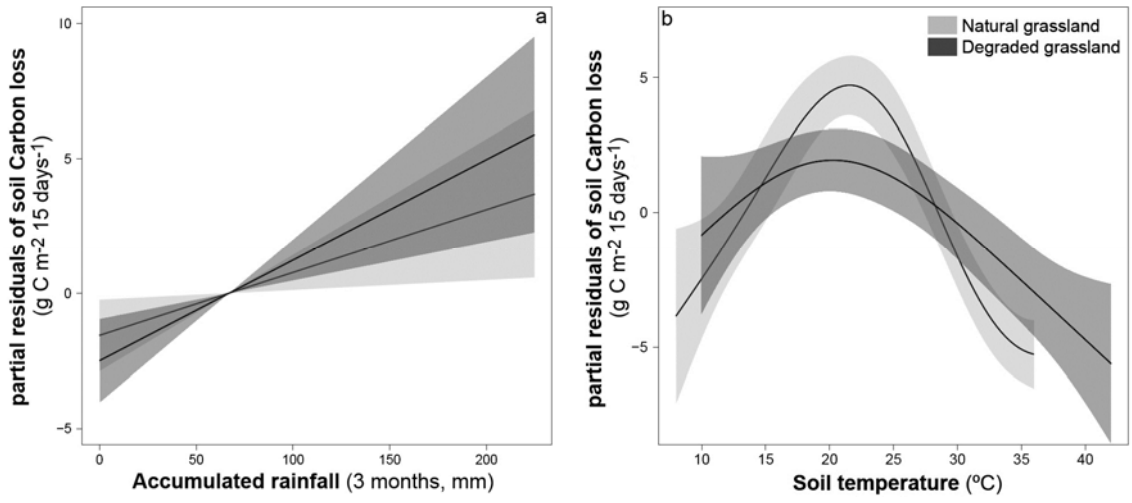


Table 1

Rainfall patterns throughout the study years (2007-2010) in the natural and degraded grasslands according to intensity and timing and soil carbon loss per year ($\text{g C m}^{-2} \text{ yr}^{-1}$). Events refer to the number of days with rainfall above 1 mm. The total soil carbon loss ($\text{g C m}^{-2} \text{ yr}^{-1}$) for 2010 is in italic because it refers to half a year only.

	YEAR			
Rainfall amount	2007	2008	2009	2010
Total rainfall (mm)	276.6	244.6	165.8	363.8
% of days with rainfall	9.9	9.0	7.4	13.2
Event frequency (%)				
1-5 mm	47.2	54.5	70.4	47.9
5-15 mm	41.7	33.3	18.5	39.6
> 15 mm	11.1	12.1	11.1	12.5
Rainfall distribution (% mm)				
1-5 mm	14.6	19.1	27.1	16.7
5-15 mm	41.9	44.8	20.5	40.4
> 15 mm	42.4	36.1	52.4	42.8
Timing (%)				
Winter	26.4	19.4	26.9	51.3
Spring	24.2	19.7	42.5	21.0
Summer	2.2	4.0	0.5	4.2
Autumn	47.2	57.0	30.1	23.6
Soil C loss (g m^{-2})				
Natural grassland	206.5	228.7	239.1	<i>148.4</i>
Degraded grassland	126.9	146.2	173.6	<i>129.2</i>

Table 2

Results of the generalised additive mixed model analysing daily soil CO₂ efflux ($\mu\text{mol m}^{-2} \text{s}^{-1}$). edf: estimated degrees of freedom for the model terms. Phenology is defined by a tensor product smoothing term (i.e., additive regression plane) using the cosine and sinus of the angular date transformation.

Effects	edf	F	P
Site (degradation level)	1	22.76	<<0.001
Soil cover	2	8.46	<<0.001
Site x Soil cover	2	3.97	0.019
Phenology	5.8	49.39	<<0.001
Soil water content (within natural grassland)	3.0	95.34	<<0.001
Soil water content (within degraded grassland)	3.0	350.47	<<0.001
Soil temperature (within natural grassland)	2.9	65.57	<<0.001
Soil temperature (within degraded grassland)	2.7	29.63	<<0.001

Table 3

Results of the generalised additive model analysing cumulative soil carbon loss ($\text{g C m}^{-2} \text{ 15 days}^{-1}$). Sample size is 160 for the four study years and two sites. edf: estimated degrees of freedom for the model terms.

Effects	edf	F	P
Site (degradation level)	1	15.76	<0.001
Accumulated rainfall in 3 months (within natural grassland)	1.0	10.68	0.001
Accumulated rainfall in 3 months (within degraded grassland)	1.0	9.51	0.002
Soil temperature (within natural grassland)	3.6	13.22	<< 0.001
Soil temperature (within degraded grassland)	2.7	5.98	0.006

SUPPLEMENTARY MATERIAL S1
Main characteristics of the study sites

<i>Variable</i>	SITE	
	NATURAL (Balsablanca)	DEGRADED (Amoladeras)
Longitude	2°1'58"W	2°15'1"W
Latitude	36°56'30"N	36°50'5"N
Altitude (m)	208	65
Orientation	NW	SW
Slope (%)	2-6	2-6
Mean annual air temperature (°C)	18	18
Mean summer air temperature (°C)	34	36
Average annual rainfall (mm)	200	200
Mean soil temperature at 3.5 cm (°C)	22.5	24.0
Mean soil water content at 3.5 cm (%)	15.2	11.7
Mean PPFD ($\mu\text{mol mol}^{-1}$)	1549	1549
Mean annual atmospheric pressure (kPa)	99	101
Maximum VPD (kPa)	4.3	4.6
Mean annual relative air humidity (%)	69.3	68.7
Vegetation	Steppe alpha grass	Steppe alpha grass
Soil type (Calcaric; WRB, 2006)	Mollic Lithic Leptosol	Lithic Leptosol
Soil texture class	Sandy loam	Sandy loam
Clay (%)	16.1	14.6
Silt (%)	22.8	27.0
Sand (%)	61.1	58.4
Bulk density (g cm^{-3})	1.25	1.11
Maximum soil depth (cm)	20	10
Vegetation cover (%)	63.2	23.1
Biological soil cover (%)	18.2	23.1
Bare soil (%)	0.3	8.1
Other cover (rock, gravel, etc.)	22.3	46.7

SUPPLEMENTARY MATERIAL S2

Spatial variability in soil properties

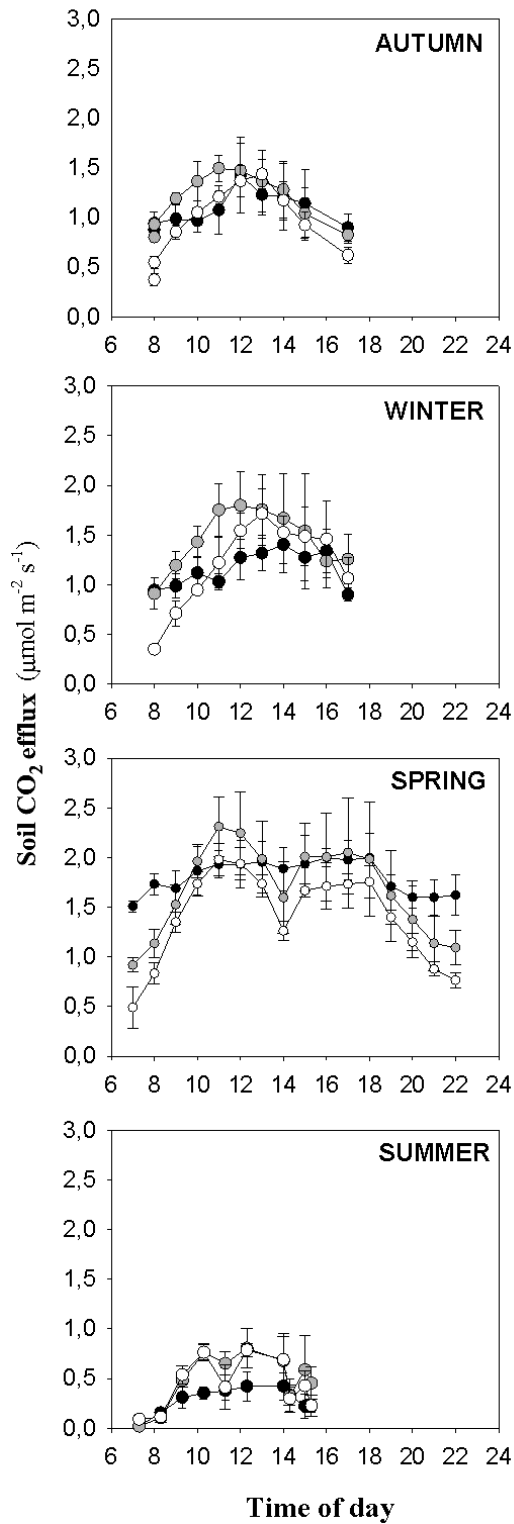
Soil properties under the three soil covers: under vegetation areas (VEG), biological soil crusts (BSC) and bare soils (BS). Values are the mean \pm 1SE ($n = 10$).

SITE	NATURAL GRASSLAND			DEGRADED GRASSLAND		
	VEG	BSC	BS	VEG	BSC	BS
Soil organic carbon (%)	2.17(0.14)	1.77(0.14)	1.63(0.14)	2.14 (0.08)	1.46(0.14)	1.33 (0.08)
Total nitrogen (%)	0.19(0.01)	0.15(0.01)	0.16 (0.01)	0.21(0.09)	0.15(0.01)	0.14 (0.01)
Bulk density (g cm ⁻³)	1.20(0.03)	1.23(0.04)	1.32(0.04)	1.21(0.02)	1.36(0.02)	1.34(0.02)
Fine root density (mg cm ⁻²)	3.30(0.44)	1.99(0.31)	2.03(0.28)	5.91(0.73)	1.30(0.24)	1.01(0.30)

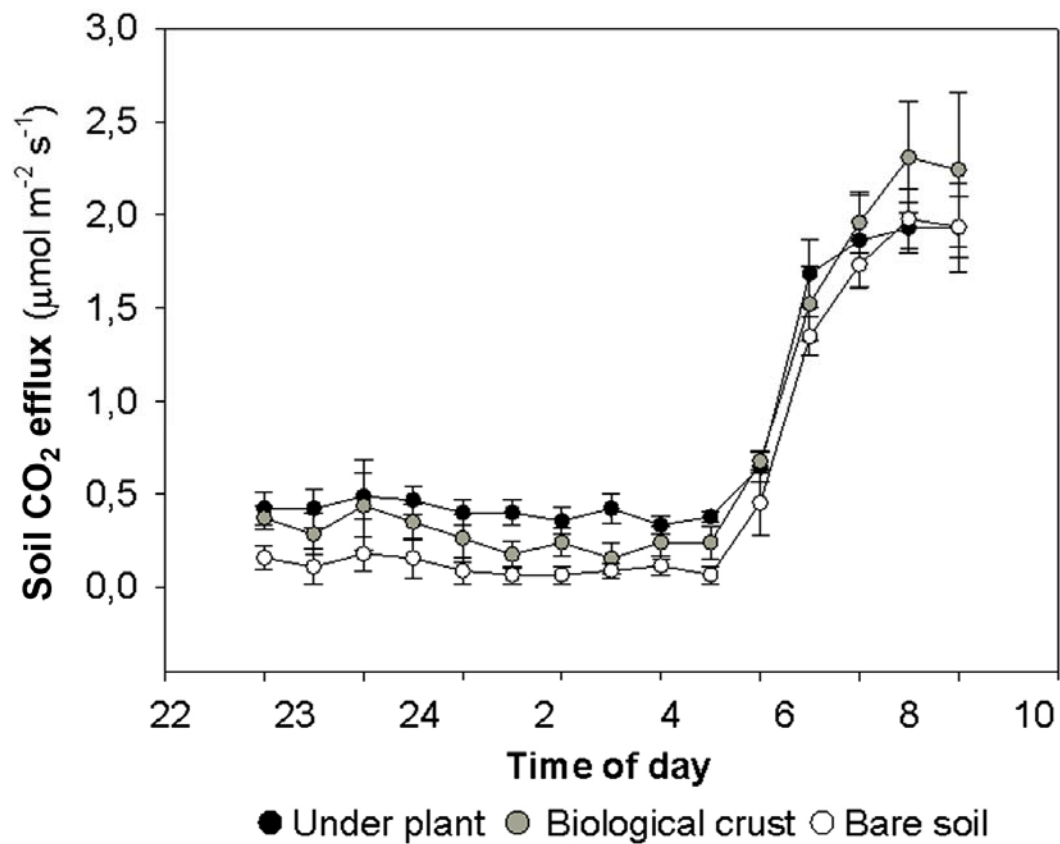
SUPPLEMENTARY MATERIAL S3

Calculation of mean daily soil CO₂ efflux rates

- (a) Diurnal course of soil CO₂ efflux ($\mu\text{mol CO}_2 \text{ m}^{-2} \text{ s}^{-1}$) in four seasons in the three soil covers, under plant, biological soil crust and bare soil ($n = 6$) measured in the natural grassland. Values are mean \pm 1 SE.



(b) Nocturnal measurements of soil CO₂ efflux ($\mu\text{mol CO}_2 \text{ m}^{-2} \text{ s}^{-1}$) made in spring in the three soil covers: under plant, biological soil crust and bare soil ($n = 6$) in the natural grassland (Balsablanca). Values are mean \pm 1SE.



According to these daily patterns, the divisors of soil CO₂ efflux rates measured in the field between 10:00 and 14:00 hours used to estimate daily averages were as follows:

	BSC	VEG	BS
Winter	2.13	1.66	2.41
Spring	1.70	1.41	1.82
Summer	2.21	2.18	2.48
Autumn	2.08	1.65	2.57

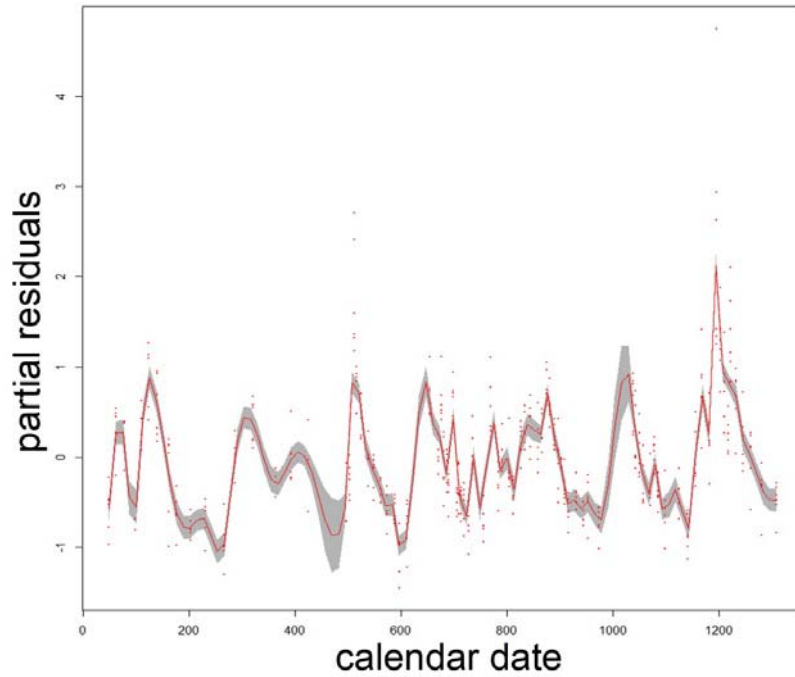
Supplementary Material S4

Interpolation method of daily measurements between sampling dates over the study period

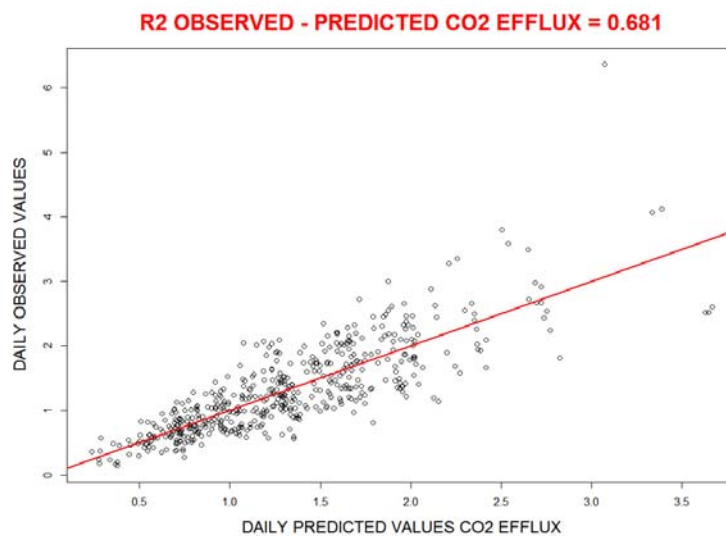
The interpolation of soil CO₂ efflux, soil temperature and soil water content is necessary in order to obtain stable averages when upscaling data to fortnights and estimate annual estimates, in order to gain insights on the role of rainfall amount on soil carbon losses. We measured these three variables intensively enough (i.e., with high frequency) to obtain reliable estimates when interpolating the data between dates. The main sort of variation would be to miss CO₂ peaks after rainfall events, that is exactly why we tried to measure always after each rainfall event as well as on a regular basis.

We applied GAMM with the available data in order to carry out the interpolation. GAMM is applied considering that (1) non-linear relationships may underline predictors-response relationships and (2) there is temporal auto-correlation in consecutive fortnights data. The predictors were *date* and the *rainfall amount of the previous day*, with calendar dates beginning on January 1st 2007 (day 1) and ending on June 30th 2010 (day 1277). The interpolation process employed using GAMMs was very robust according to the predictive power of the six models applied to data for the two sites (degraded and natural grasslands) and three soil covers (vegetation patches, biological soil crust, and bare soil). All models accounted for an extremely high proportion of deviance (always > 75%).

The test of predictive power was carried out by means of jackknifing. Thus, we carried out the GAMMs many times for each site-soil cover not using one particular sample in each model. That sample was predicted by the GAMM that used the remaining samples. This process was repeated as many times as the number of sample units, in such a way that every sample unit is predicted without being used in the modelling process. The following figure shows the result of the “worst” GAMM model applied to the data of Balsablanca (natural grassland), using only the samples of the collars in the vegetation patches. The pseudo-R² of the GAMM was 0.746. The little red dots show the residuals for each one of the 516 soil CO₂ efflux measurements of six collars obtained in 86 sampling dates. The R² of that model is only 74.6% due to the relatively high sample variance among soil collars within each date, probably related to “microsite” differences between collars regarding vegetation, slope, soil characteristics, insolation related to cardinal position of collars around vegetation patches, etc. Nevertheless, the averages of the six collars for each sampling date follow a tight pattern with only relatively high uncertainty (see the amplitude of the shaded areas) when consecutive sampling dates are more than 20 days apart.

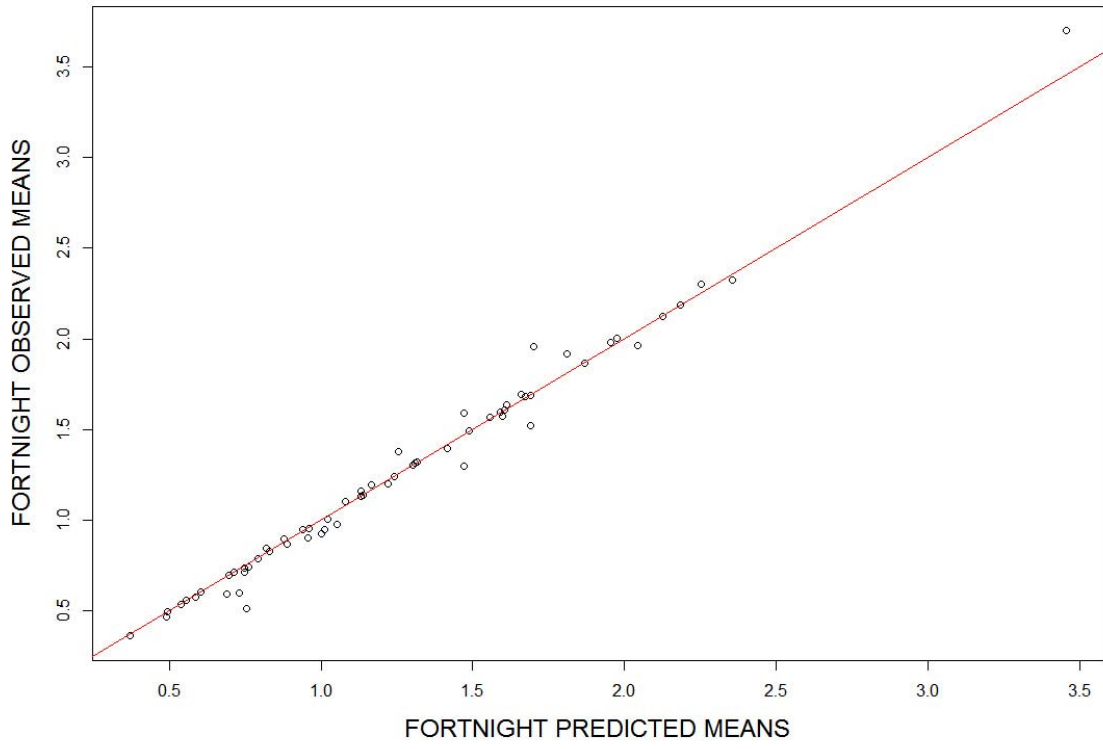


The relationship between the observed (actual) and predicted soil CO₂ efflux estimates for each collar in each sampling date obtained in the jackknife procedure is shown in the next figure.



The R^2 of that relationship (68.1%) is lower than the pseudo- R^2 of the GAMM model, but high enough considering that it is strictly a predictive analysis considering all the variability among soil collars and dates. But this result does not pose any important concern, as our interpolation has been made for fortnights, averaging the predictions of the six collars in the days included in the fortnight. If we consider the sampling days within every fortnight, the averages of the measured rates and the averages of the jackknife-predictions are tightly correlated in the corresponding fortnights. This is clearly shown in the next Figure.

R2 OBSERVED - PREDICTED = 0.987



SUPPLEMENTARY MATERIAL S5

Alternative GAMMs to those presented in Tables 2 and 3

Alternative generalised additive mixed models to that presented in Table 2, regarding daily soil CO₂ efflux ($\mu\text{mol m}^{-2} \text{s}^{-1}$). edf: estimated degrees of freedom for the model terms. Seasonality is defined by a tensor product smoothing term (i.e., additive regression plane) using the cosine and sinus of the angular date transformation.

Soil water content and soil temperature not nested within Sites

Effects	edf	F	P
Site (degradation level)	1	24.41	<<0.001
Soil cover	2	8.41	<<0.001
Site x Soil cover	2	2.97	0.052
Seasonality	5.7	76.58	<<0.001
Soil water content	3.0	422.08	<<0.001
Soil temperature	3.0	76.57	<<0.001

Substitution of soil water content by rainfall amount and rainless duration

Effects	edf	F	P
Site (degradation level)	1	61.67	<<0.001
Soil cover	2	7.09	0.001
Site x Soil cover	2	0.67	0.512
Seasonality	5.8	33.23	<<0.001
Rainfall amount (natural grassland)	1.0	41.91	<<0.001
Rainfall amount (degraded grassland)	2.8	12.42	<<0.001
Rainless duration (natural grassland)	2.9	20.92	<<0.001
Rainless duration (degraded grassland)	2.9	9.33	<<0.001
Soil temperature (natural grassland)	3.0	56.70	<<0.001
Soil temperature (degraded grassland)	2.8	18.07	<<0.001

Alternative generalised additive mixed model to that presented in Table 3, regarding cumulative soil carbon loss ($\text{g C m}^{-2} 15 \text{ days}^{-1}$). Sample size is 160 for the four study years and two sites. edf: estimated degrees of freedom for the model terms.

Substitution of Accumulated rainfall in 3 months by fortnight soil water content

Effects	edf	F	P
Site (degradation level)	1	7.87	0.006
Average fortnight soil water content (within natural grassland)	1.1	1.71	0.168
Average fortnight soil water content (within degraded grassland)	1.7	3.93	0.018
Soil temperature (within natural grassland)	3.6	9.32	<< 0.001
Soil temperature (within degraded grassland)	2.6	4.52	0.023